(NASA-CR-164321) APPLICATION OF VARIABLE STRUCTURE SYSTEM THEORY TO AIRCRAFT FLIGHT CONTROL Interim Report (Drexel Univ.) 42 p HC A03/MF A01 CSCL 01C

N81-23093

Unclas

G3/08 42390

Application of Variable Structure System Theory to Aircraft Flight Control

Interim Report

May, 1981

Research Supported by N.A.S.A. Ames Research Center, NASA Grant No. NAG 2-8[†]

Principal Investigator: Dr. Anthony J. Calise

Investigator: Dr. Isaac Kadushin

Research Assistant: Mr. Fred Kramer

Mechanical Engineering & Mechanics Department

Drexel University

Philadelphia, PA 19104

[†] The AV-8A portion of this research is partially supported by the Naval Air Systems Command.

CONTENTS

NOMENCLATURE

A	=	plant matrix
B	=	control matrix
d	=	localizer beam error, m
N_h (RN)	=	engine RPM, %
q	=	pitch rate increment, rad/s
s	=	distance from the sliding surface, s
t	=	time, s
u	=	surge velocity in body frame, m/s
v	=	inertial velocity increment, m/s
w	=	heave velocity in body frame, m/s
x	=	state vector
α	=	angle of attack increment, rad
γ	=	flight path angle increment, rad
δ_e	=	elevator angle (longitudinal stick) increment, deg (in)
δ_T	=	throttle increment, deg
ζ	=	damping ratio
$\eta(\nu)$	=	nozzle angle increment, rad
θ	=	pitch angle increment, rad

1. Introduction

This report summarizes the current status of our research on the application of Variable Structure System (VSS) theory tc design aircraft flight control systems. Two aircraft types are currently being investigated: the Augmentor Wing Jet STOL Research Aircraft (AWJSRA), and AV-8A Harrier. The AWJSRA design considers automatic control of longitudinal dynamics during the landing phase. The main task for the AWJSRA is to design an automatic landing system that captures and tracks a localizer beam. The control task for the AV-8A is to track velocity commands in a hovering flight configuration. Much of the effort since our last report [1] has been devoted to developing computer programs that are needed to carry out VSS design in a multivariable frame work, and in becoming familiar with the dynamics and control problems associated with the aircraft types under investigation. Numerous VSS design schemes were explored, particularly for the AWJSRA. The approaches presented here are the ones that appear to be the best suited for these aircraft types. Examples are given of the numerical results currently being generated. A brief summary of VSS theory was presented in [1].

2. Glide Slope Control For The Augmentor Wing Jet STOL Research Aircraft (AWJSRA)

2.1 The System

The AWJSRA is a research aircraft modified from the De Havilland C-8-A turboprop by modifying the wing to include an augmentor flap system, boundary layer control and other lift augmentation systems, and by replacing the turboprop engine by a split flow jet engine. The system has been described in [2, 3, 4]. The purpose of the present work was to design a precise glide slope control system invariant to changes in some of the aircraft parameters.

2.2 Control System Design

The control system was designed to use the existing controls: elevator angle and the engine thrust - an independent system controlled by the throttle. The jet nozzle was set to a nominal value of 90°. The equilibrium trajectory was chosen to be a 7.5° glide at 30.9 m/sec (60 knots) starting at an altitude of 396.5 m (1300 ft). Other system parameters are given in [3,4]. The design was based on the linearized model in [4] modified to a wind axis coordinate system:

$$\dot{x} = Ax + Bu \tag{2.1-1}$$

where

$$x^T = [d,\ 100\ \theta,\ 100\ \alpha,\ v,\ 100\ q,\ N_h] \tag{2.1-2}$$

$$u^T = [100\ \delta v,\ 100\ \delta_e,\ \delta_T] \tag{2.1-3}$$

$$A = \begin{bmatrix} 0 & -.309 & .309 & 0 & 0 & 0 \\ 0 & 0 & 0 & 0 & 1 & 0 \\ 0 & .042 & -.52 & -.94 & 1.03 & -.36 \\ 0 & -.097 & .043 & -.052 & .0007 & 0 \\ 0 & .0174 & -.0816 & .004 & -1.36 & 0 \\ 0 & 0 & 0 & 0 & 0 & -1 \end{bmatrix} \tag{2.1-4}$$

$$B = \begin{bmatrix} 0 & 0 & 0 \\ 0 & 0 & 0 \\ 0 & 0 & 0 \\ -.015 & 0 & 0 \\ 0 & 1.2 & 0 \\ 0 & 0 & .72 \end{bmatrix} \tag{2.1-5}$$

At the equilibrium trajectory, the nozzle is perpendicular to the aircraft's longitudinal axis. Thus nozzle angle variation is a rather poor velocity control, as can be seen from the small value of the control derivative. It was, therefore, decided to keep the nozzle angle constant.

The variable structure control requires controls capable of almost instantaneous changes. The only fast control available in the AWJSRA is the elevator angle. The engine thrust control has a time constant of about 1 sec. The control system consists of two loops: the first loop is an internal loop with state variables [θ, α, v, q] controlled by the elevator angle δ_e and designed as a variable structure control system [5, 6]. This is mainly an attitude control system. Speed control is achieved through changes in angle of attack. The control system parameters were determined by placement of the eigenvalues at the desired position when the system is in sliding mode along the surface

$$s = C_1 (100\ \theta) + C_2\ (100\ \alpha) + C_3\ v + (100\ q) = 0 \qquad (2.2)$$

The eigenvalues were placed so that the resulting inner loop system will have natural frequency of 1.5 rad/sec, damping ratio $\zeta = 0.7$ and a real eigenvalue of $0.1\ \text{sec}^{-1}$. The resulting sliding surface is

$$s = +\ 3.82\,(100\ \theta) - 2.22\ (100\ \alpha) - 0.934\ v\ + (100\ q) = 0 \qquad (2.3)$$

and the resulting closed loop system, in sliding mode is:

$$\begin{bmatrix} 100\ \dot{\theta} \\ 100\ \dot{\alpha} \\ \dot{v} \end{bmatrix} = \begin{bmatrix} -3.82 & 2.22 & .934 \\ -3.88 & 1.77 & .67 \\ -.33 & .148 & -.05 \end{bmatrix} \begin{bmatrix} 100\ \theta \\ 100\ \alpha \\ v \end{bmatrix} + \begin{bmatrix} 0 \\ 0 \\ -.36 \end{bmatrix} \delta N_h \qquad (2.4)$$

with q determined from (2.3);

$$100q = -3.82\ (100\ \theta) + 2.22\ (100\ \alpha) + 0.934\ v \qquad (2.5)$$

The velocity control through attitude can be seen by considering the changes in θ, α, and q required to counter a change in v, so that s=0. As can be seen from (2.3), a positive v can be obtained by a decrease in α, and vice versa.

The use of a variable structure control system in sliding mode for the attitude control makes the aircraft control invariant to changes in the coefficients of the state matrix governing the pitch rate, q.

These coefficients depend on the position of the airplane c.g.. Thus, the AWJSRA control will be invariant to changes in the c.g position. Such a feature may be important for future applications of the variable structure control to airplanes with large c.g. variation such as transport and military flying vehicles.

The outer loop control system consists of the "beam error" control effected through thrust variation. As the thrust direction in steady state is practically perpendicular to the flight path, changes in thrust cause changes in the vertical acceleration and, thus induce changes in angle of attack. As a result, a change in flight path angle occurs. Since beam error is proportional to γ , this error is eliminated after a transient motion. Changes in α also cause changes in aircraft attitude and velocity. These are controlled by the inner loop, which is in sliding mode along the surface s. The engine rpm, which controls the thrust is in turn controlled by the throttle and is unaffected by other state variables.

The outer loop was designed under the assumption that the inner loop is already in the sliding mode. Thus, the variable q was eliminated using (2.5). The new state vector is thus

$$x_1^T = [d,\ 100\ \theta,\ 100\ \alpha,\ v,\ \delta N_h] \tag{2.6}$$

and the equations of motion for $100\ \dot{\theta}$, $100\ \dot{\alpha}$, $\dot{v}$ are those of (2.4).

The outer control loop was designed by minimizing the quadratic performance index

$$J = 1/2 \int_{T_s}^{\infty} [x_1^T Q\ x_1 + \delta_e^2]\ dt \tag{2.7-1}$$

with

$$Q = \begin{bmatrix} 10 & 0 & 0 & 0 & 0 \\ 0 & 1 & 0 & 0 & 0 \\ 0 & 0 & 1 & 0 & 0 \\ 0 & 0 & 0 & 1 & 0 \\ 0 & 0 & 0 & 0 & 10 \end{bmatrix} \tag{2.7-2}$$

and T_s is the time at which the sliding mode begins.

The resulting throttle control is:

$$\delta_{th} = - C_1 x_1 \tag{2.8}$$

with

$$C_1 = [5.53, -6.09, 5.27, -5.91, -4.8] \tag{2.9}$$

2.3 Sliding Motion Results

The system dynamics described in (2.2) were simulated in the sliding mode, using a second order Runge-Kutta method. The system was required to decrease a 10m. initial beam error. The results are shown in Figures 2.1 to 2.6. The beam error decreased to 5% of its initial value in about 11 seconds (see Fig. 2.1). There was practically no overshoot. The motion towards the equilibrium glide path was accompanied by a slight nose down pitching (Fig. 2.2) and a very small increase in velocity (Fig. 2.4). The main effect was a considerable increase in thrust as can be seen from the increase in r.p.m. (Fig. 2.5). This is the main path control and according to [2,3] is preferred by human pilots. The nose down tilt required to hold the speed approximately constant is also described in [3,4]. Such a control technique, which couples speed, attitude, and path control may be a heavy burden on the human pilot and, therefore, degrade his rating (opinion) of the system. However, the automatic control system is fully capable of both path, attitude, and speed control regardless of their coupling.

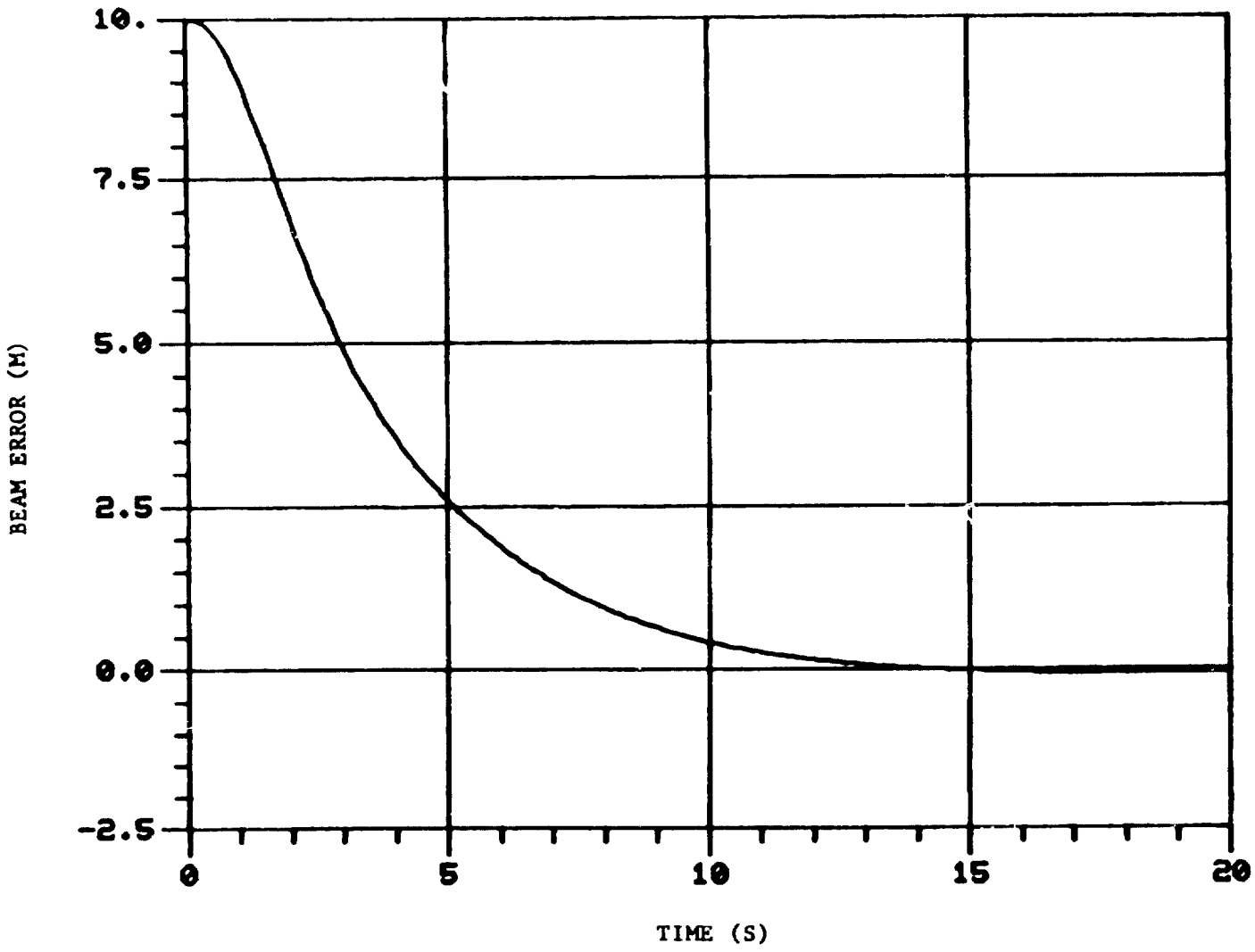

FIGURE 2.1 The Variation of the Beam Error with Time.
(The attitude control system in sliding mode)

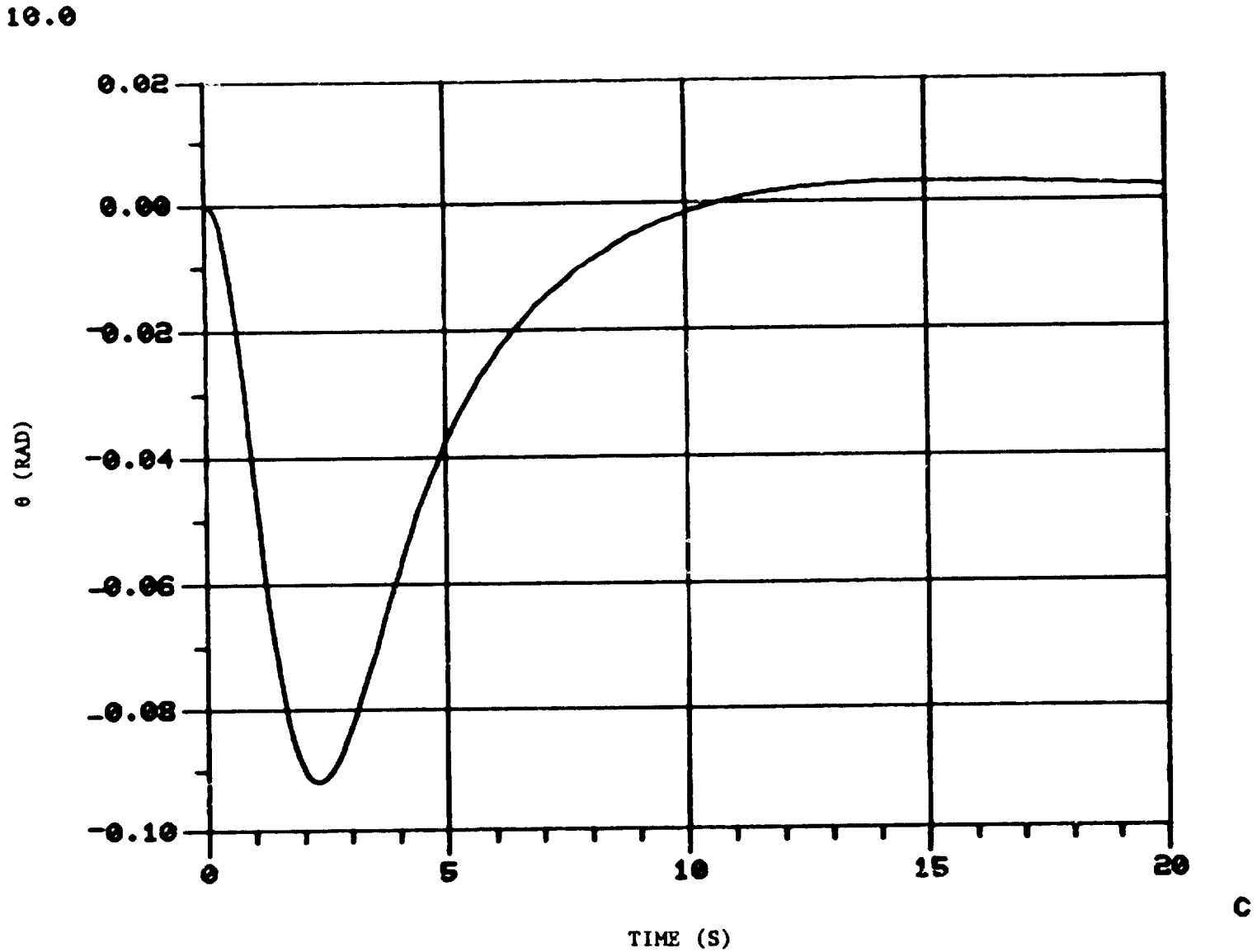

FIGURE 2.2. Variation in θ Due to Beam Error Control
(The attitude control system in sliding mode)

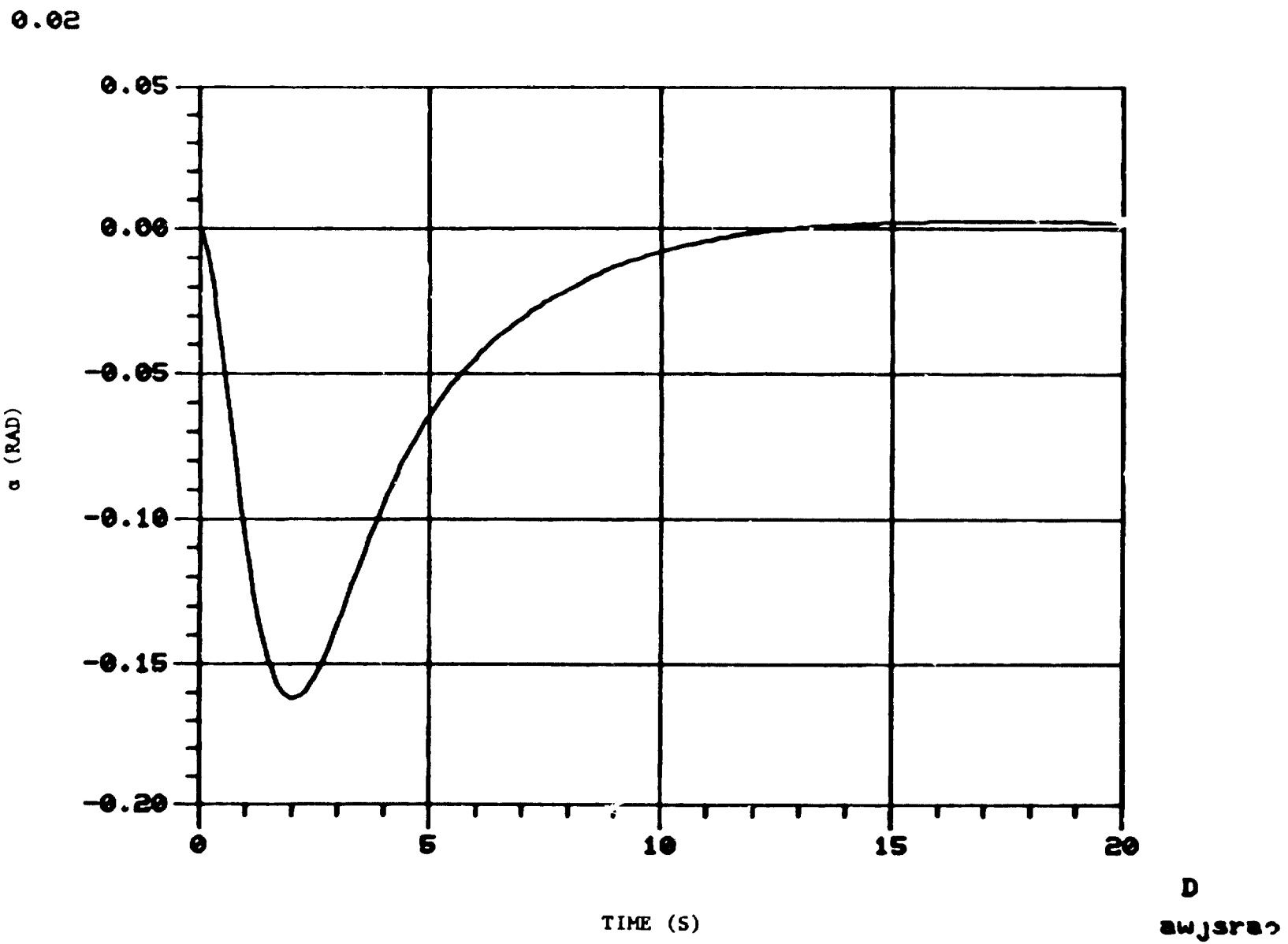

FIGURE 2.3 Variation in Angle of Attack Due to Beam Error Control
(The attitude control system in sliding mode)

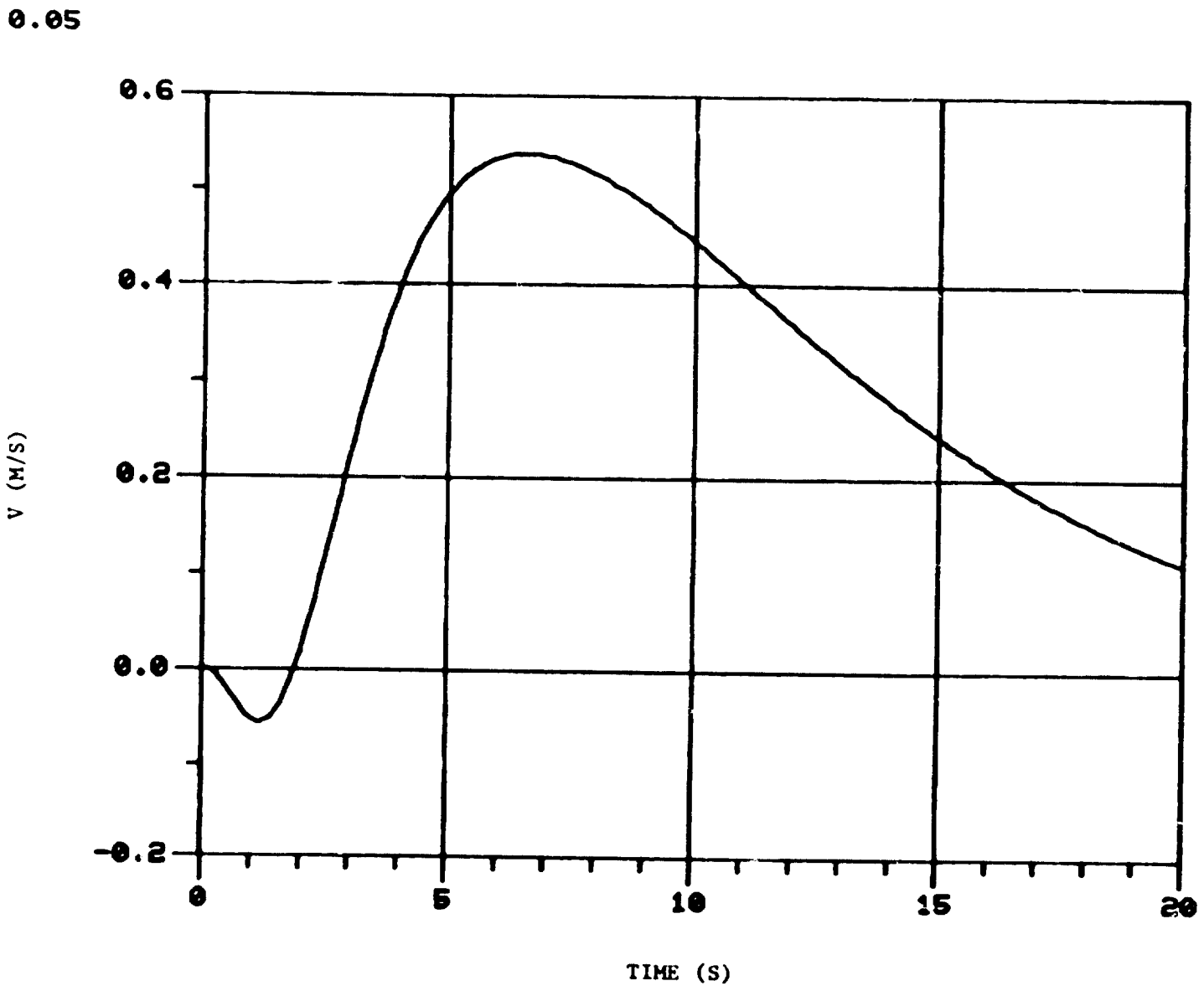

FIGURE 2.4 Variation in Velocity
(The attitude control system in sliding mode)

0.6

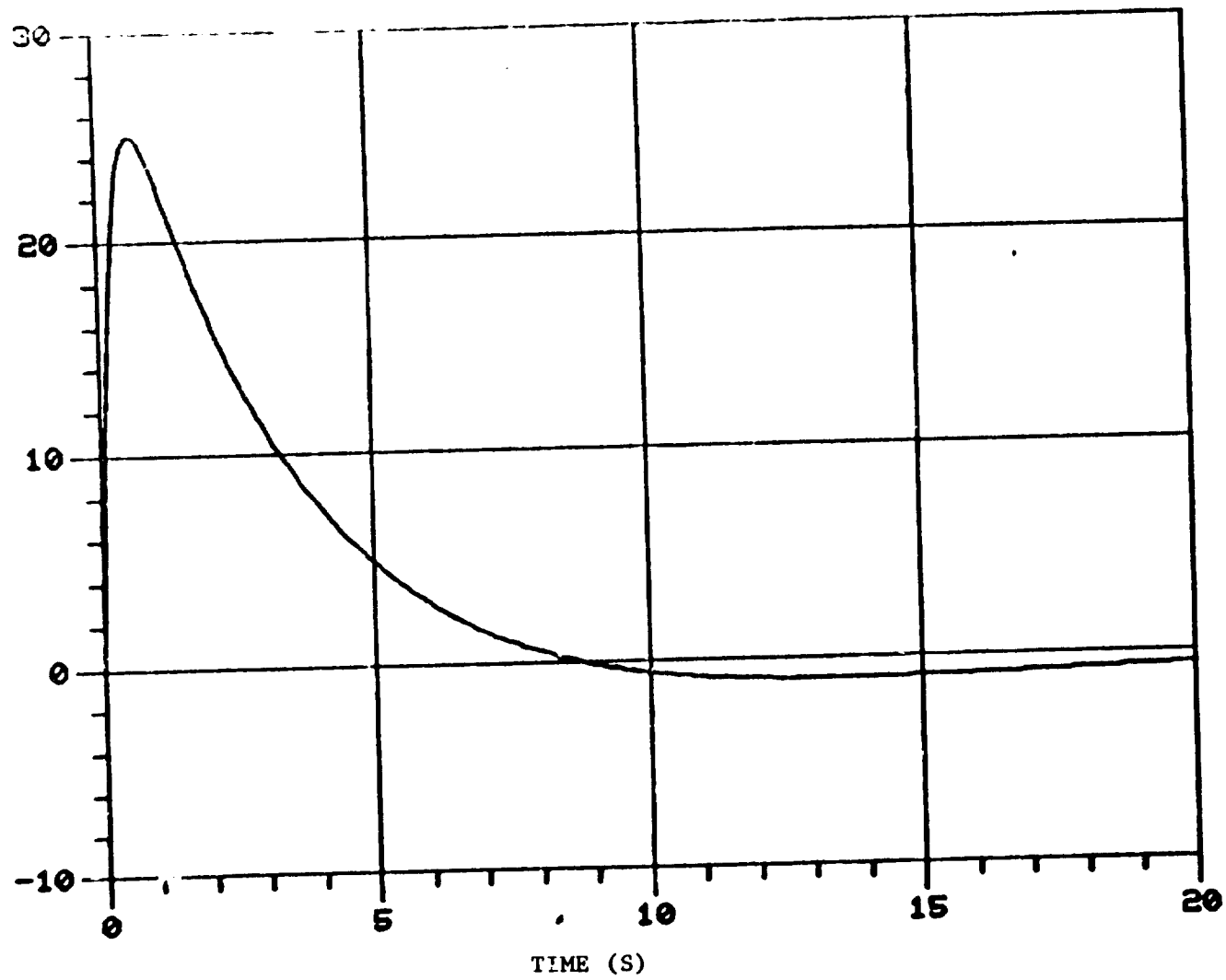

F

awjsr3o

FIGURE 2.5 Engine RPM Variation Required For Beam Error Control.
(The attitude control system in sliding mode)

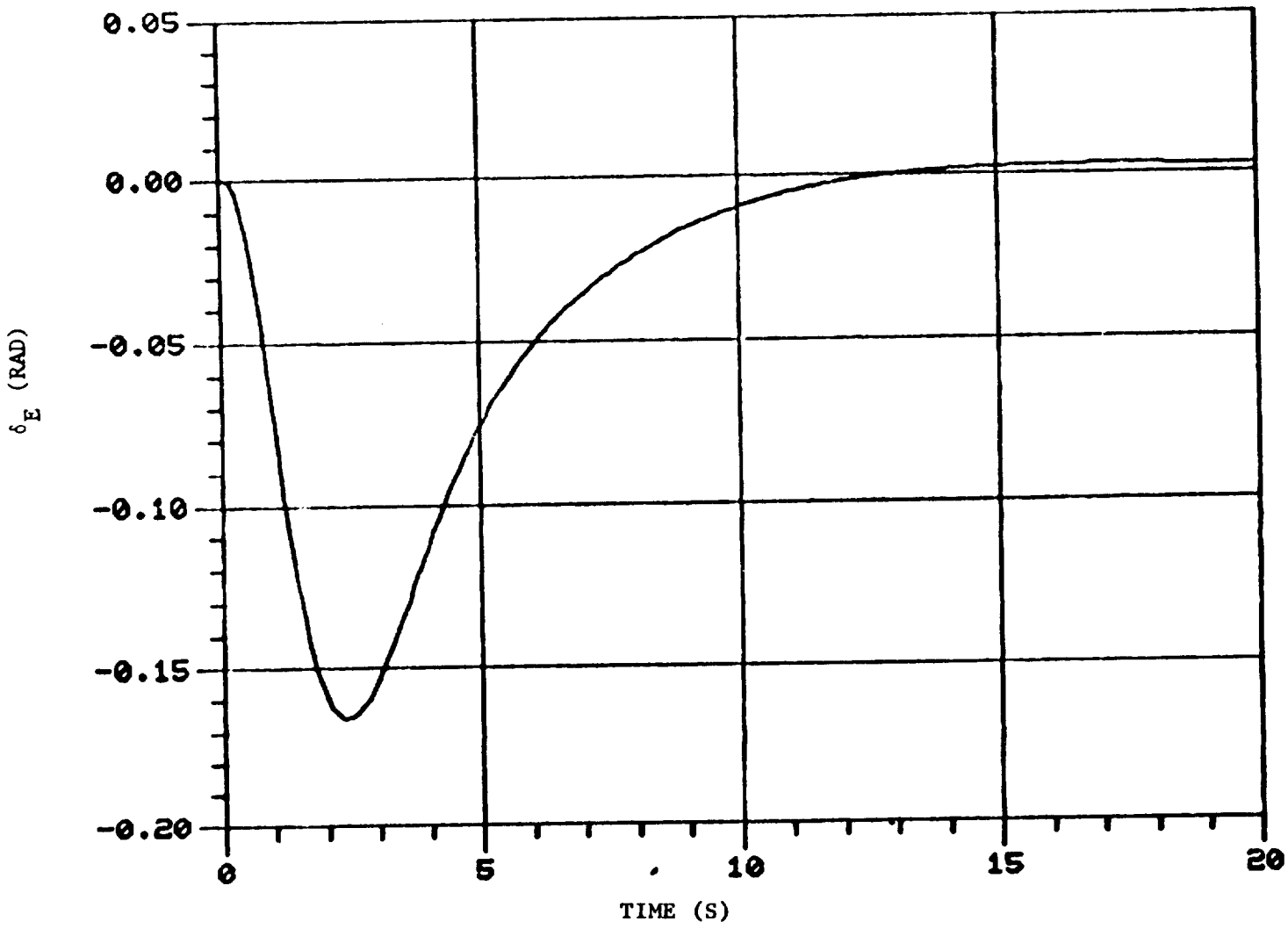

FIGURE 2.6 Elevator Angle Variation During Beam Error Control.
(The attitude control system in sliding mode)

2.4 Design of Controls Required for Reaching the Sliding Surface

The design procedure for reaching the sliding surface is described in [1, 5]. The requirement is that the norm of s should always decrease, i.e.,

$$s\dot{s} < 0 \tag{2.10}$$

The procedure described in [1] was generally used, however, since the rpm factor N_h influences the motion of the inner loop variables, an additional component had to be added to the control, as shown in Chapter VIII of [5]. From (2.1) and (2.3), we obtain

$$s\dot{s} = s[\sum_{i=1}^{6} a_i x_i - 1.2\ \delta_E] \tag{2.11}$$

where

$$\begin{aligned} a_1 &= 0 & a_4 &= 2.14 \\ a_2 &= .0147 & a_5 &= .173 \\ a_3 &= 1.03 & a_6 &= .8 \end{aligned} \tag{2.12}$$

To satisfy (2.10), the following control structure is appropriate:

$$\delta_E = -\sum_{i=1}^{6} \psi_i x_i \quad ; \quad \psi_i = \begin{cases} \alpha_i , & sx_i > o \\ \beta_i , & sx_i < o \end{cases} \tag{2.13}$$

where

$$-\alpha_i > a_i/1.2 \quad , \quad -\beta_i < a_i/1.2 \tag{2.14}$$

The following selection was made:

$$\begin{aligned} \alpha_1 &= 0 & \beta_1 &= 0 \\ \alpha_2 &= .02 & \beta_2 &= 0 \\ \alpha_3 &= 1.6 & \beta_3 &= 0 \\ \alpha_4 &= 3.6 & \beta_4 &= 0 \\ \alpha_5 &= 0.3 & \beta_5 &= 0 \\ \alpha_6 &= 1.3 & \beta_6 &= 0 \end{aligned} \tag{2.15}$$

The aircraft and control system dynamics both off and on the sliding surface were simulated and the results are shown in Figures 2.7 - 2.13. The response is initially slower due to a throttle command limit that was imposed such that $\delta_T < 10.7°$, which corresponds to $N_h = 98.5$ (normal take-off power setting). The general motion is similar to that of ideal sliding, with the exception that δ_e is no longer continuous (Fig. 2.13). The beam error (Fig. 2.7) settles in 14 seconds and is accompanied by small changes in α (Fig. 2.8), nose down pitching (Fig. 2.9) and minor velocity variations (Fig. 2.10). The engines RPM response is given in Fig. 2.11, and exhibits the effect of limiting δ_T. The value of s during the run is shown in Fig. 2.12. Note that sliding occurs almost immediately and is maintained throughout the maneuver.

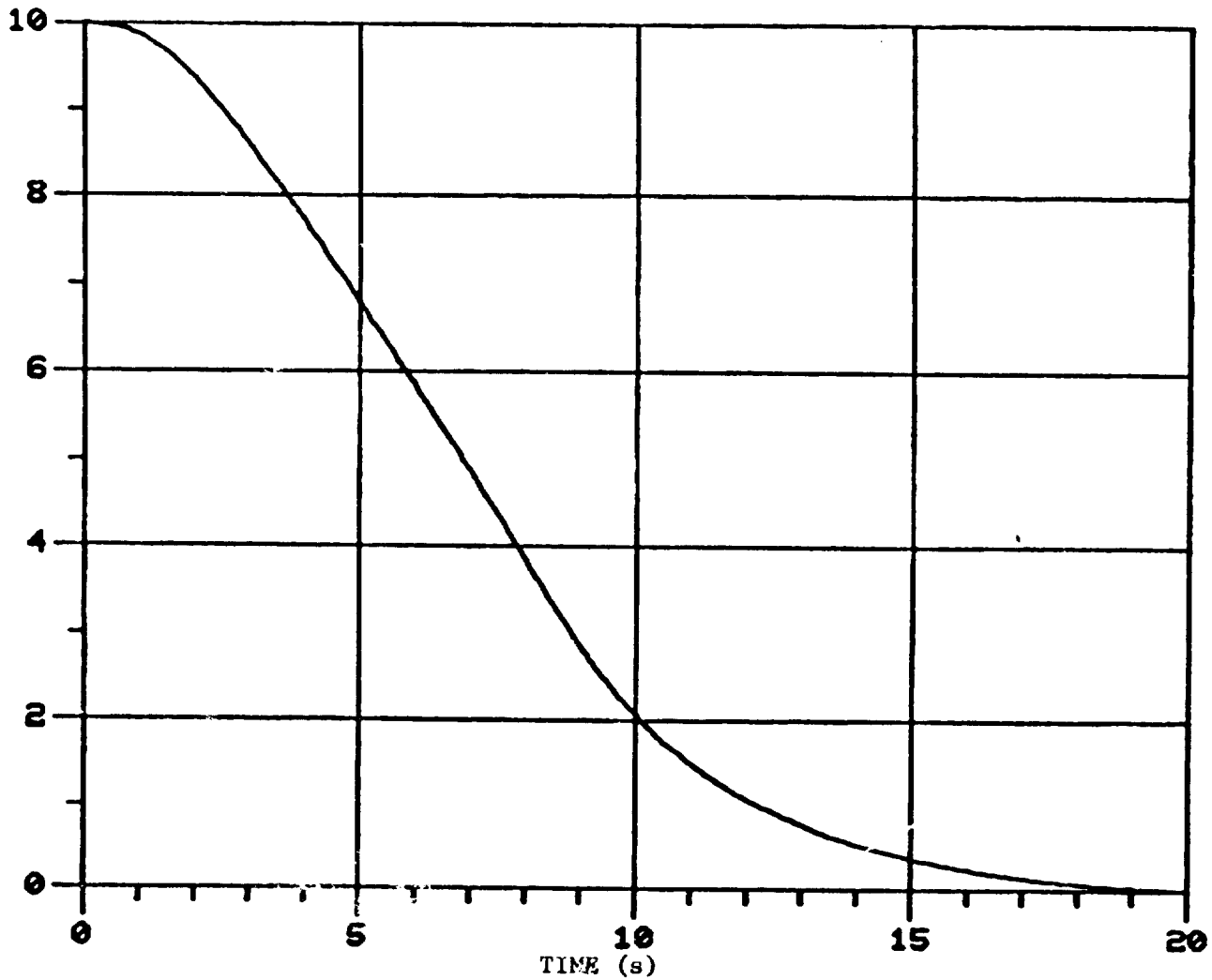

Figure 2.7 Beam Error Variation with Time.

B

awjsrao.vssl.

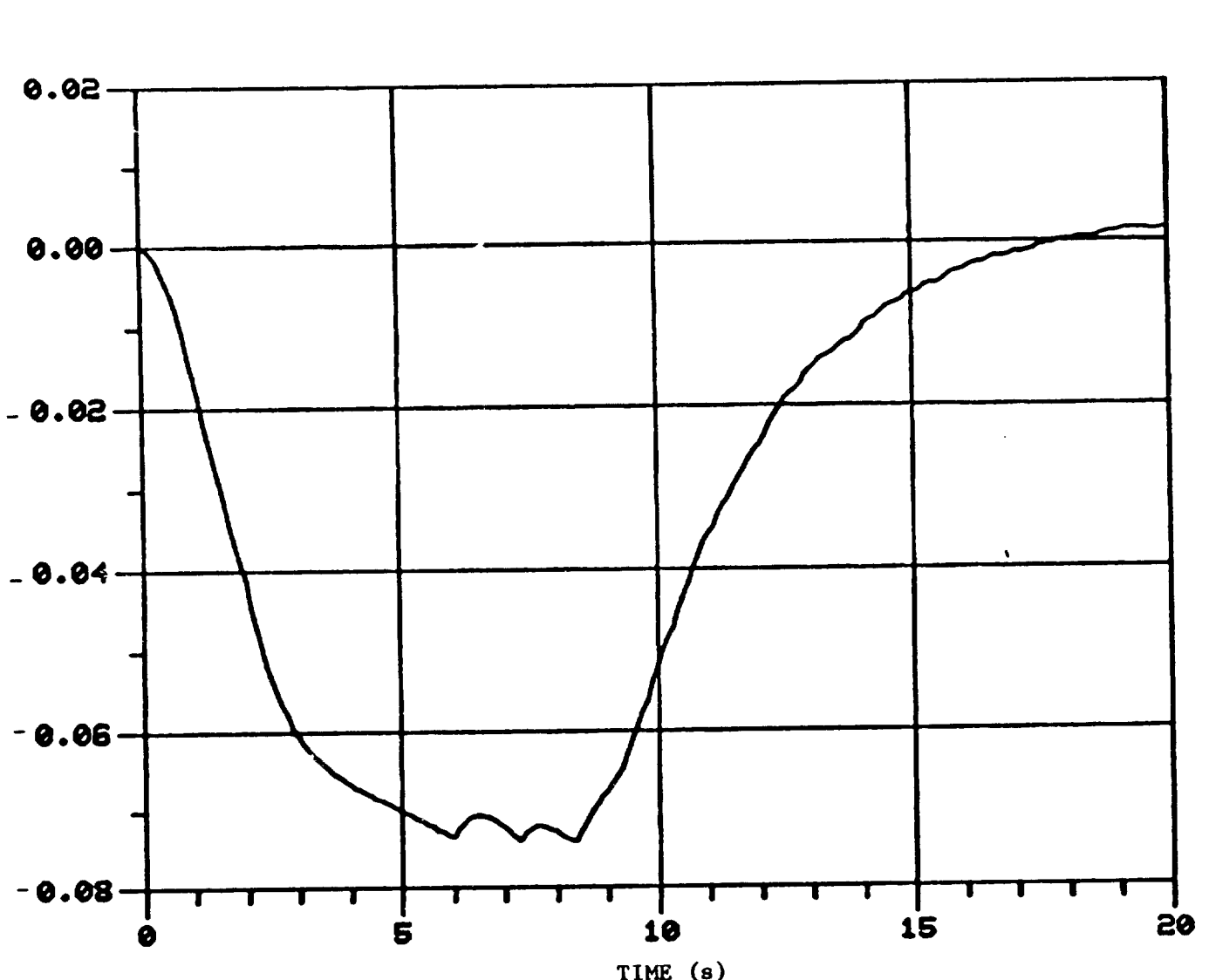

Figure 2.8 Angle of Attack Variation due to an Initial Beam Error of 10 m.

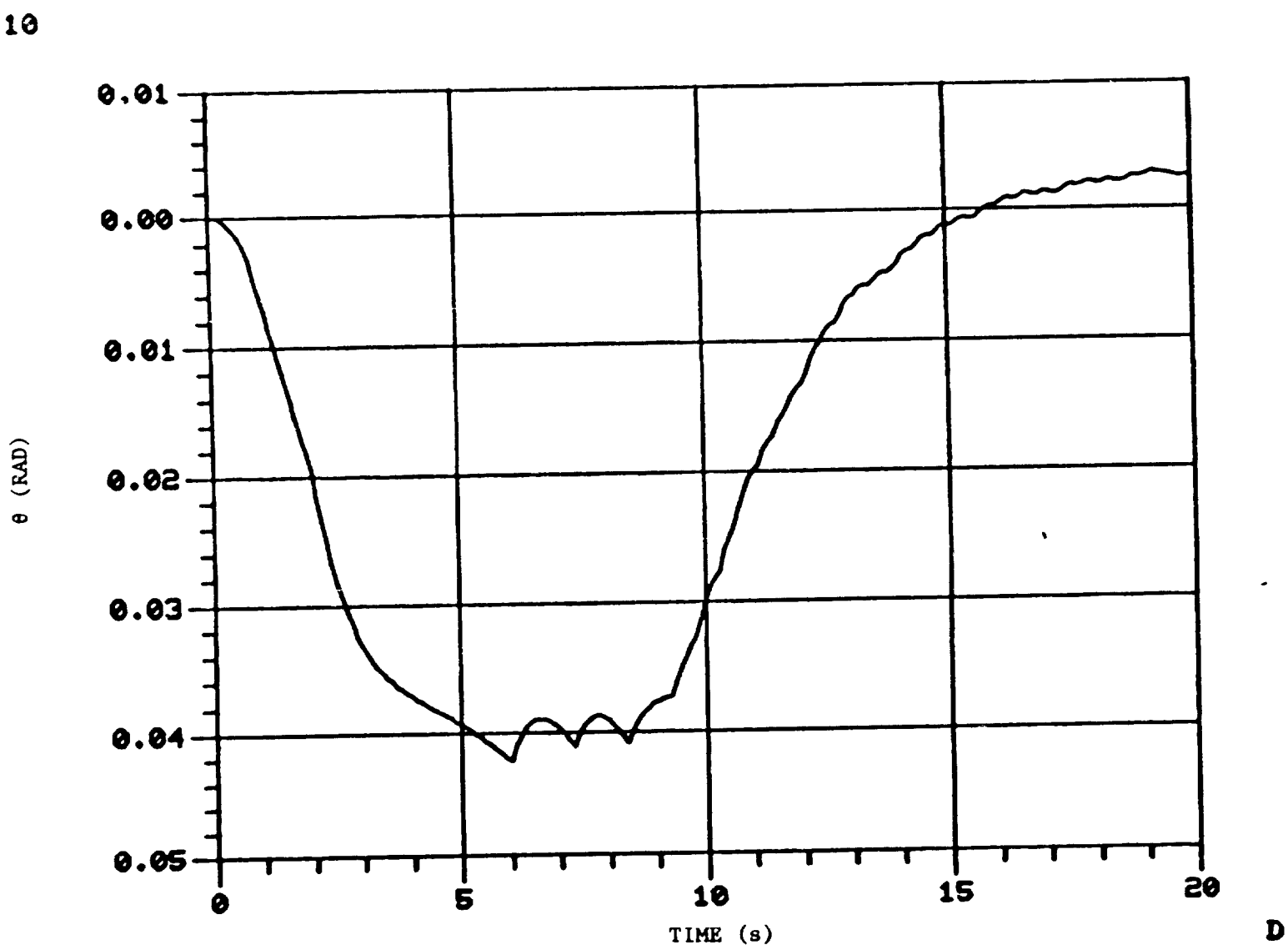

Figure 2.9 Pitch Angle Variation due to an Initial Beam Error of 10 m.
awjsrao.vssi.s03

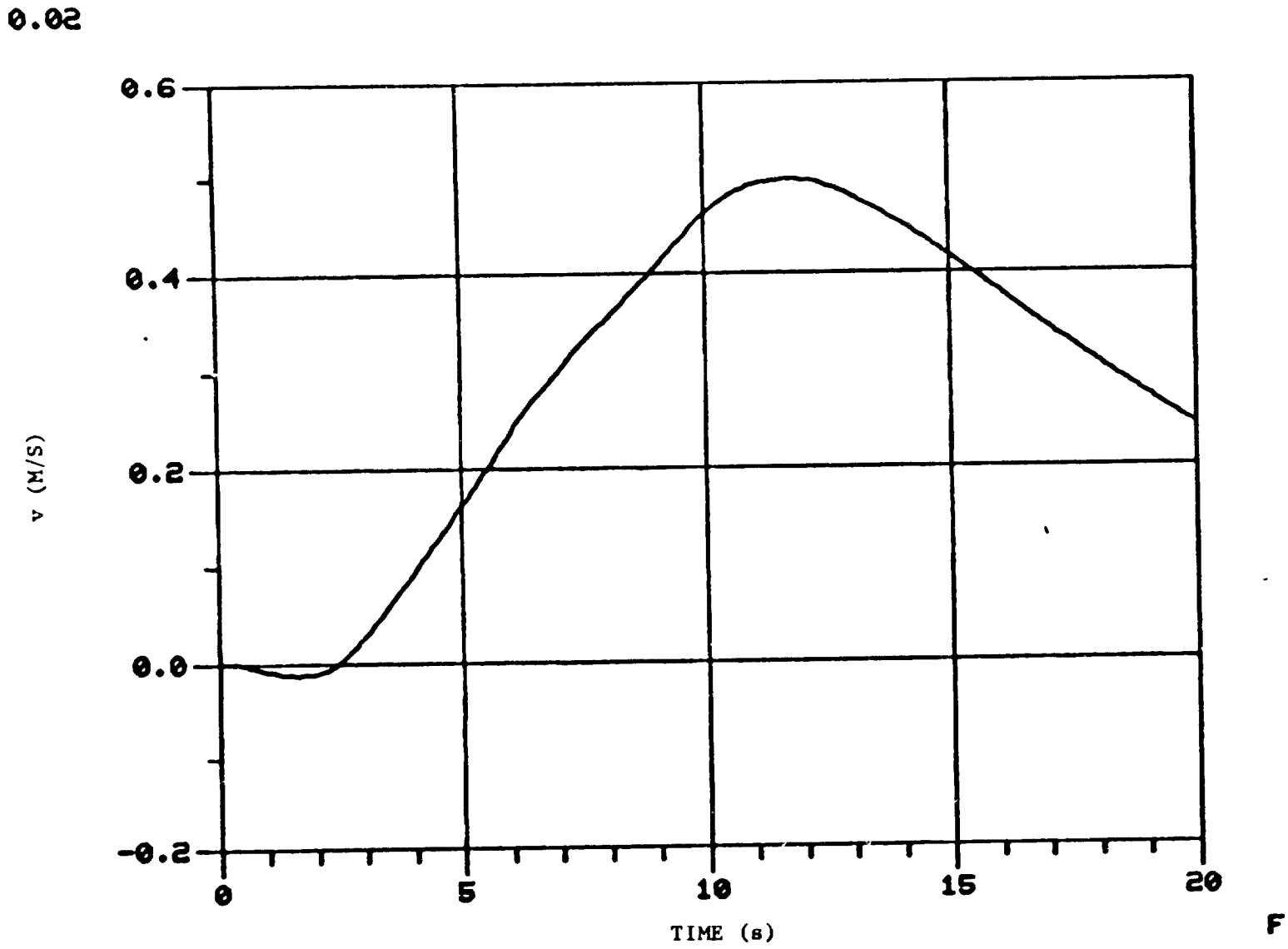

Figure 2.10 Velocity Variation due to an Initial Beam Error of 10 m.
awjsrao.vss1.s03

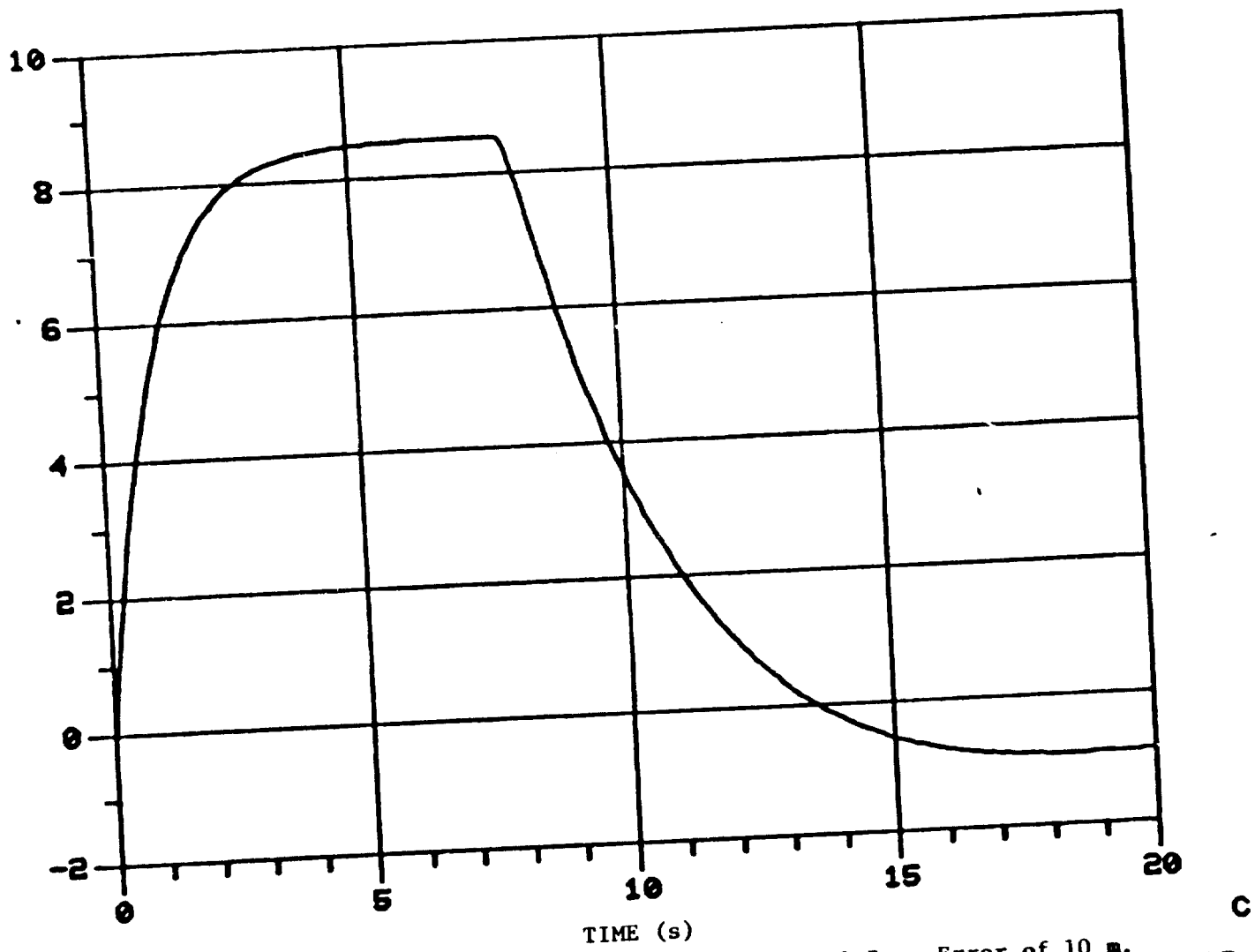

Figure 2.11 Engine RPM Variation due to an Initial Beam Error of 10 m.
awjsrao.vss1.s03

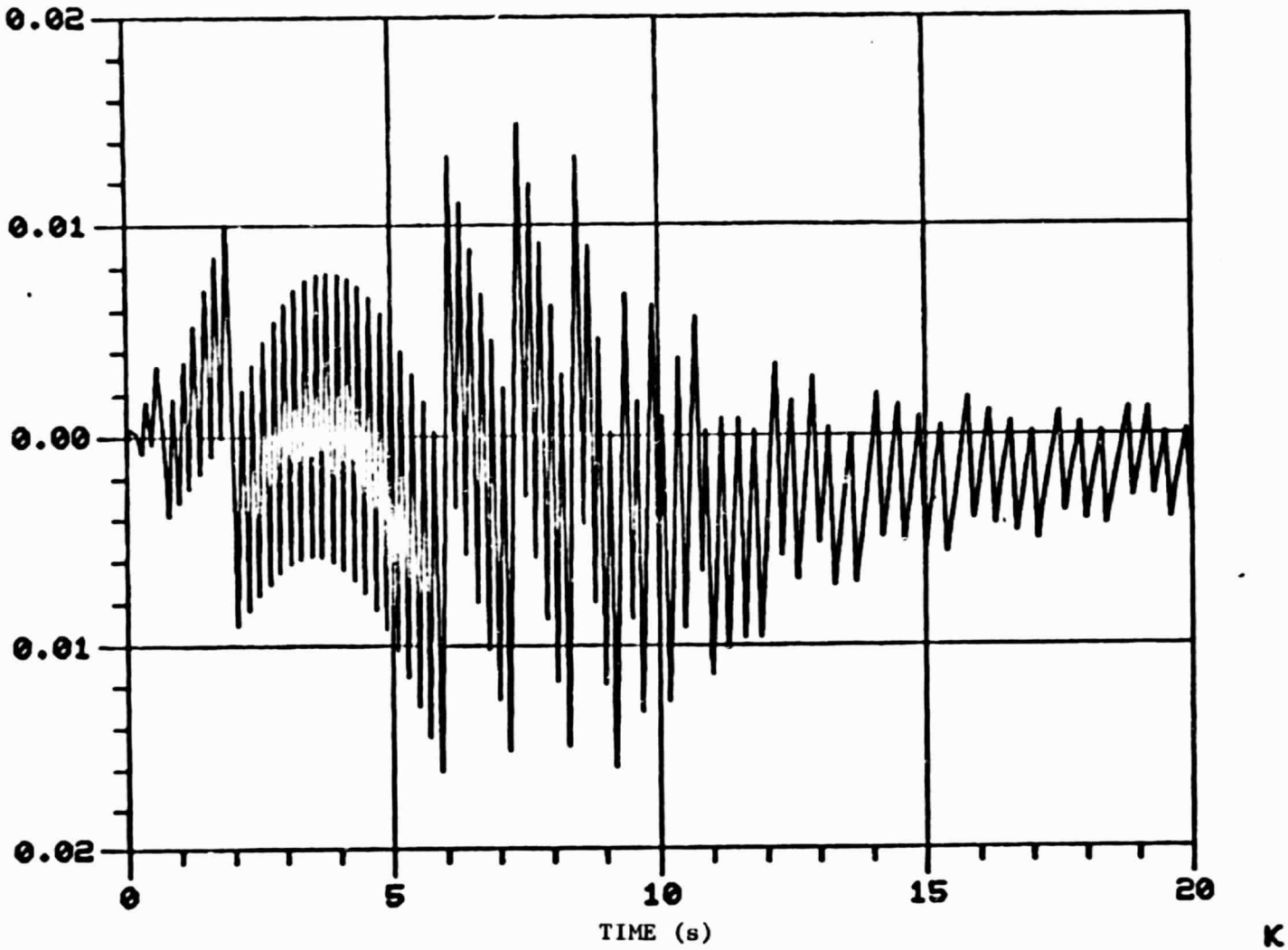

Figure 2.12 Changes in the Sliding Surface Value During Beam Error Control awjsrao.vss1.s03

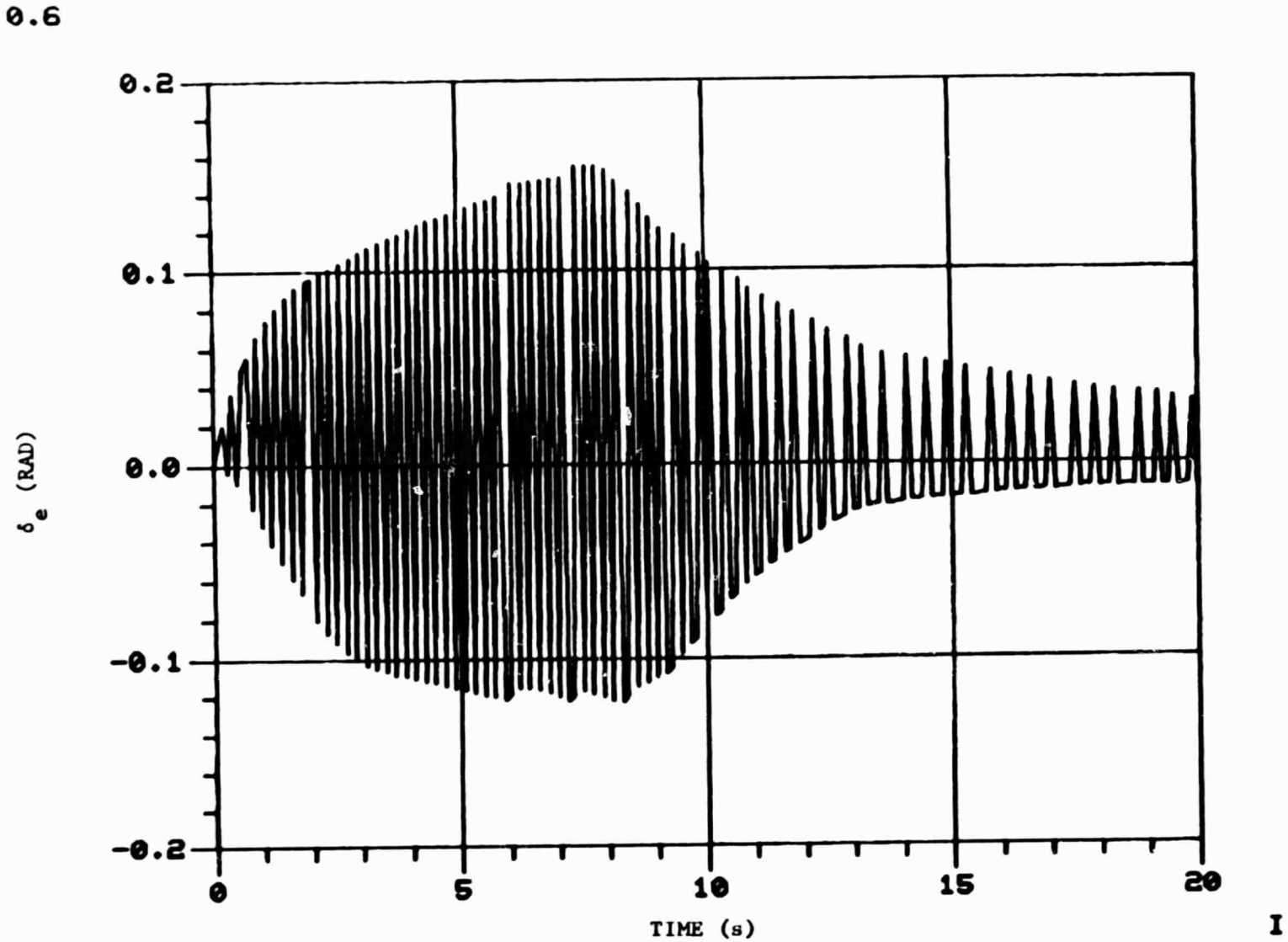

Figure 2.13 Elevator Variation due to an Initial Beam Error of 10 m.

awjsrao.vssi.s03

3. VSS Design For The AV-8A

This portion of our research considers the VSS design of a velocity command control system for the AV-8A in hovering flight. Both longitudinal and lateral dynamics will be considered, however, this report will only address control of the longitudinal velocity components (surge and heave).

Reference [6] gives the linearized model for the Harrier dynamics for airspeeds between 0 and 120 knots. We have elected to use the values for 30 knots, which result in the following model for the system dynamics in the body frame:

$$\dot{x} = Ax + Bu \tag{3.1}$$

where

$$x^T = [u,\ w,\ \theta,\ q,\ RN] \tag{3.2}$$

$$u^T = [\delta_e\ ,\ \eta\ ,\ RN_c] \tag{3.3}$$

$$A = \begin{bmatrix} -.035 & -.02 & -9.8 & 0 & .002 \\ -.011 & -.105 & -1.66 & 0 & -.309 \\ 0 & 0 & 0 & 1 & 0 \\ .0056 & 0 & 0 & -.13 & .0016 \\ 0 & 0 & 0 & 0 & -4.86 \end{bmatrix} \tag{3.4}$$

$$B = \begin{bmatrix} 0 & -9.8 & 0 \\ .16 & .28 & 0 \\ 0 & 0 & 0 \\ .2 & 0 & 0 \\ 0 & 0 & 4.86 \end{bmatrix} \tag{3.5}$$

In the design nozzle angle is held fixed (η=0), so that the only means of achieving a u_c is by pitching the aircraft. Vertical velocity is controlled by RN_c. In the design of systems with a command input, it is customary to redefine the state and control perturbations about a commanded equilibrium state and control obtained by setting $u = u_c$, $w = w_c$ and solving for the remaining states and controls by equating (3.1) to zero. This detail is omitted here but the definitions are implied.

3.1 VSS Design of the Attitude Loop

The VSS design for attitude control is based on the controller structure shown in Figure 3.1. The sliding surface is defined by:

$$s = C_1 \, \delta\theta + q \quad , \quad \delta\theta = \theta - \theta_c \tag{3.6}$$

where

$$\theta_c = k_1 \, \delta u \quad , \quad \delta u = u - u_c \tag{3.7}$$

and u_c is regarded as a constant or slowly varying input. In sliding mode (s=o) we have from (3.4) and (3.6)

$$\tau_1 \, \dot{\theta} = -\theta + \theta_c \quad , \quad \tau_1 = 1/C_1 \tag{3.8}$$

which is stable for any $C_1 > 0$. The transient response is dictated by C_1 and is invariant with respect to remaining state variables. The design of k_1 and C_1 is based on Fig. 3.2. The closed loop poles were chosen from Fig. 3.3 taken from [7]. Selecting $\omega_n = 2$ rad/s and a damping parameter of 3 $\sec^{-1}$ (which corresponds to $\zeta = .75$), the resulting values for C_1 and k_1 are:

$$C_1 = 3.0 \ \ s^{-1} \ \ ; \ \ k_1 = .136 \ \ s/m \tag{3.9}$$

The heaving motion is controlled using a conventional proportional control law

$$RN_c = .1378 \, w - .8 \, RN \tag{3.10}$$

To guarantee reaching and existance of the sliding mode, it is sufficient that

$$s\dot{s} < 0 \tag{3.11}$$

Differentiating (3.6) and assuming $\dot{u}_c = 0$, we obtain

$$s\dot{s} = s\left[\sum_{i=1}^{5} a_i \, x_i + .2 \, \delta_e\right] \tag{3.12}$$

where

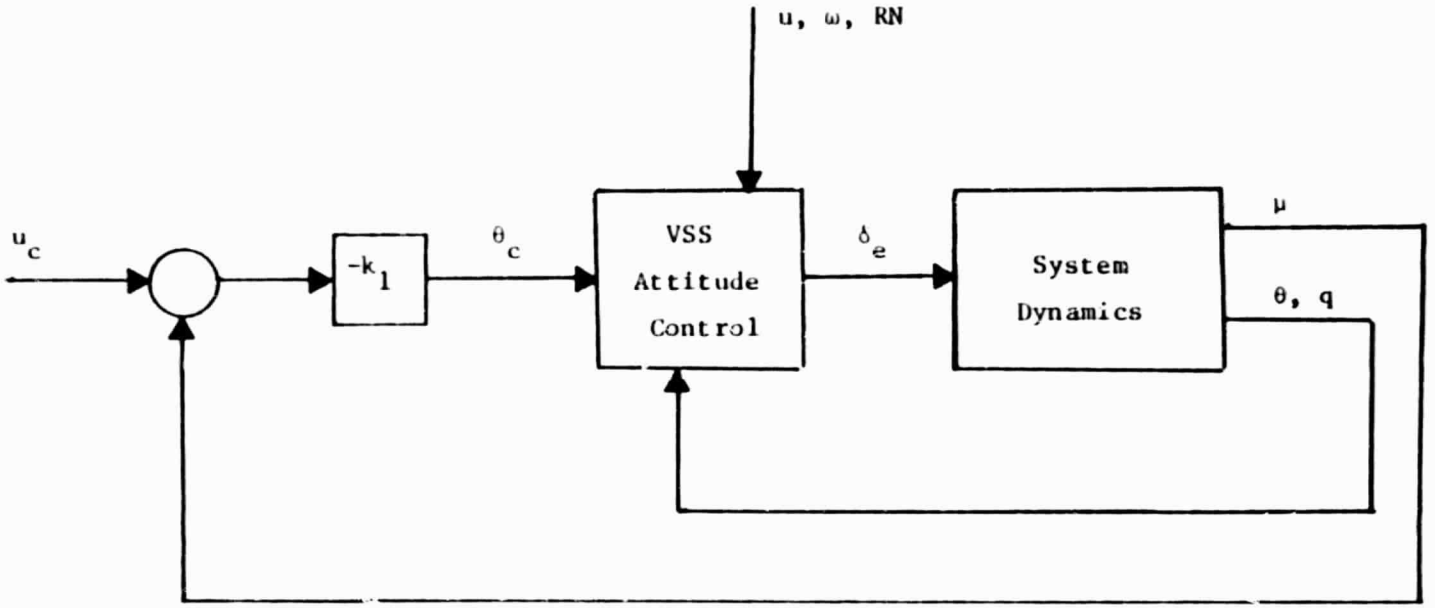

Figure 3.1 Controller Structure for Surge Dynamics

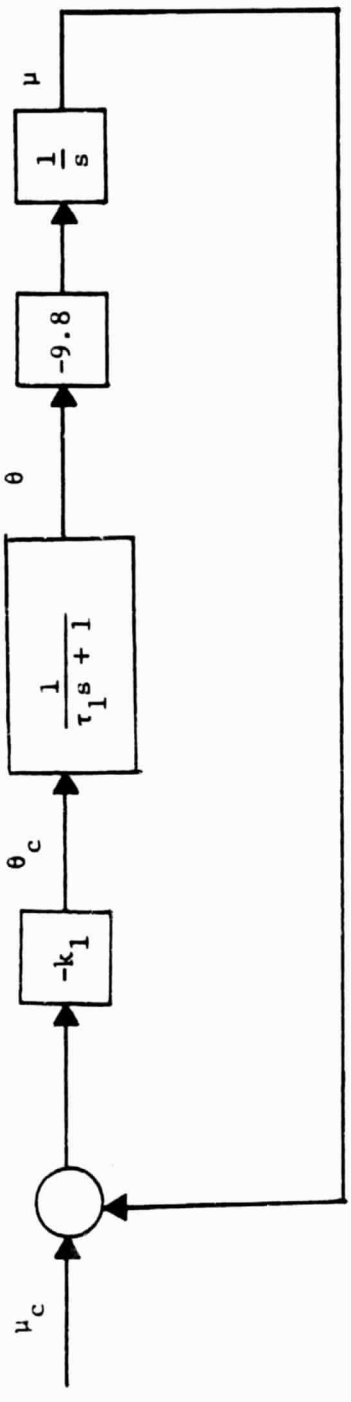

Figure 3.2 Approximate Model for Surge Dynamics in Sliding Mode.

VTOL DYNAMIC STABILITY

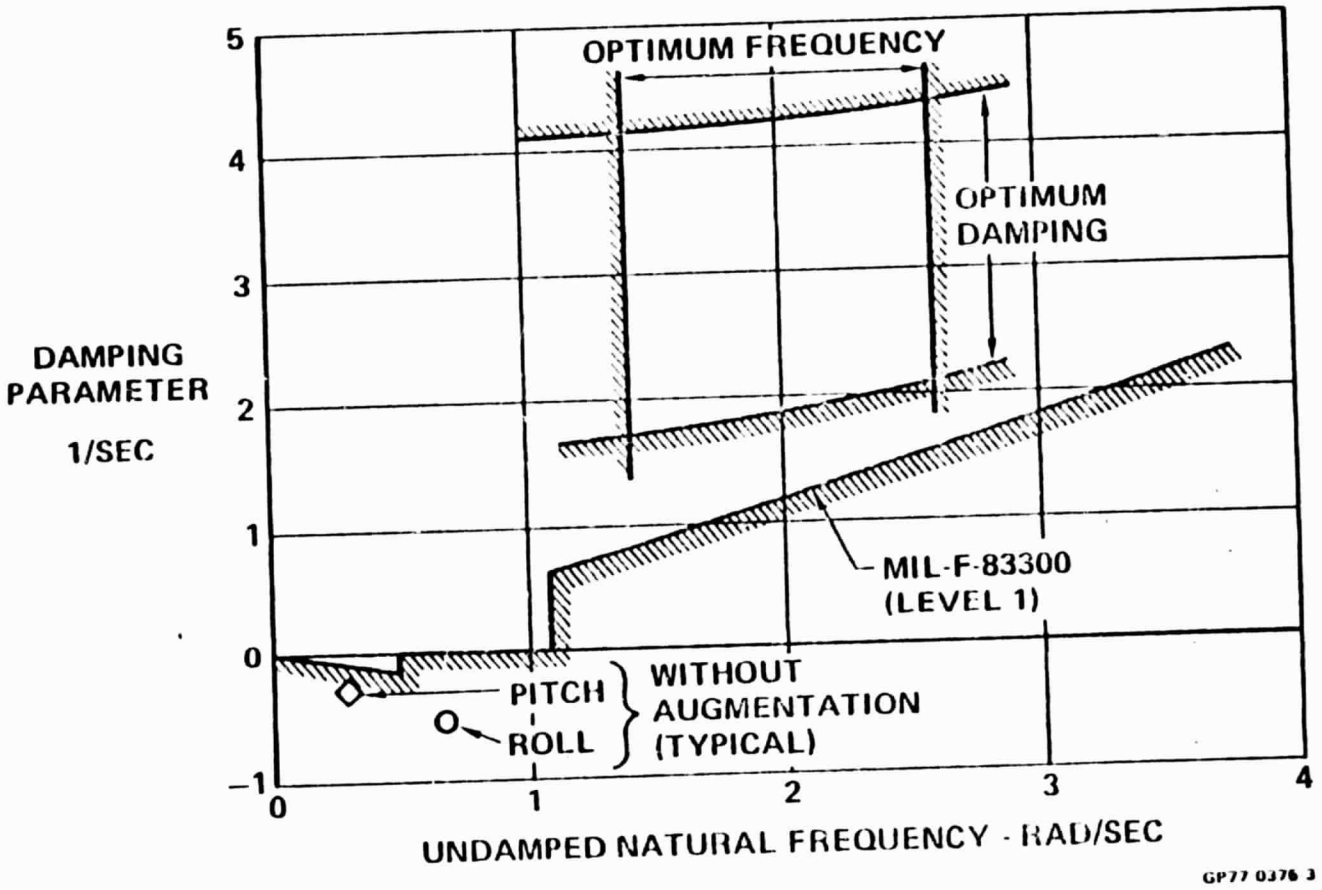

Figure 3.3 Damping and Frequency Bands for Optimum Handling Quality in VTOL Hovering Flight.

$$a_1 = .0056 + C_1 k_1 (0.35) \qquad a_4 = C_1 - .13$$

$$a_2 = .014 + C_1 k_1 (.02) \qquad a_5 = .0016 - C_1 k_1 (.002)$$

$$a_3 = C_1 k_1 (9.8)\ \theta \tag{3.13}$$

To satisfy (3.11), the following control structure is used

$$\delta_e = -\sum_{i=1}^{5} \psi_i x_i - k_s s \quad ; \quad \psi_i = \begin{cases} \alpha_i , & s x_i > o \\ \beta_i , & s x_i < o \end{cases} \tag{3.14}$$

where

$$\alpha_i > a_i/.2 \quad , \quad \beta_i < a_i/.2 \tag{3.15}$$

Allowing for possible variations in the parameters in (3.4) with the exception of A(1,3), the following selections were made

$$\alpha = \begin{matrix} .200 \\ .222 \\ 20.4 \\ 15.0 \\ .008 \end{matrix} \qquad \beta = \begin{matrix} 0 \\ 0 \\ 19.6 \\ 13.7 \\ 0 \end{matrix} \tag{3.16}$$

The last term in (3.14) basically controls the time required to reach the sliding surface, and k_s was chosen as 4.0 in-s.

3.2 Comparison to a Conventional Design

A conventional design of the attitude loop for the control structure of Figure 3.2 follows the same lines except that the transfer function for $\theta_c \rightarrow \theta$ is second order

$$\frac{\theta(s)}{\theta_c(s)} = \frac{.2\ k_2}{s^2 + (.13 + .2k_3) + .2\ k_2} \tag{3.17}$$

where

$$\delta_e = -k_2\ (\theta - \theta_c) \ - k_3\ q \tag{3.18}$$

Placing the closed loop poles to match the response time of the variable structure system we obtain

$$k_1 = .0816 \text{ s/m}$$

$$k_2 = 50 \text{ in}$$

$$k_3 = 24.35 \text{ in-s}^2 \qquad (3.19)$$

Note that the gains in (3.19) are considerably higher than the gains in (3.14) for the variable structure control in the vicinity of the sliding surface (s=0). This should aid in avoiding control saturation and instability due to large command inputs.

3.3 Numerical Results

The numerical results of this section compare the VSS control to a conventional control design for response stability under the presence of saturating control. The magnitude of δ_e was limited to 4 inches. Two levels of responses are given, corresponding to initial velocity errors of -3 m/s and -10 m/s. Figures 3.4 to 3.7 give the VSS response for an initial velocity error of -3 m/s. Note from Fig. 3.6 that sliding initiates at 2.5 seconds, when the response is essentially complete. Figure 3.7 shows that there is little coupling with the heave dynamics. Figures 3.8 to 3.10 give the velocity pitch attitude, and longitudinal stick responses for an initial velocity error of -10 m/s. Note the similarity of response in velocity with that of Fig. 3.4.

Figures 3.11 - 3.14 show the velocity and longitudinal stick responses with proportional control for the same conditions. Note that for an initial velocity error of -10 m/s, the proportional control is on the verge of instability, exhibiting 25% overshoot and prolonged periods of control saturation. Figures 3.13 and 3.14 should be compared with Fig. 3.8 and Fig. 3.10.

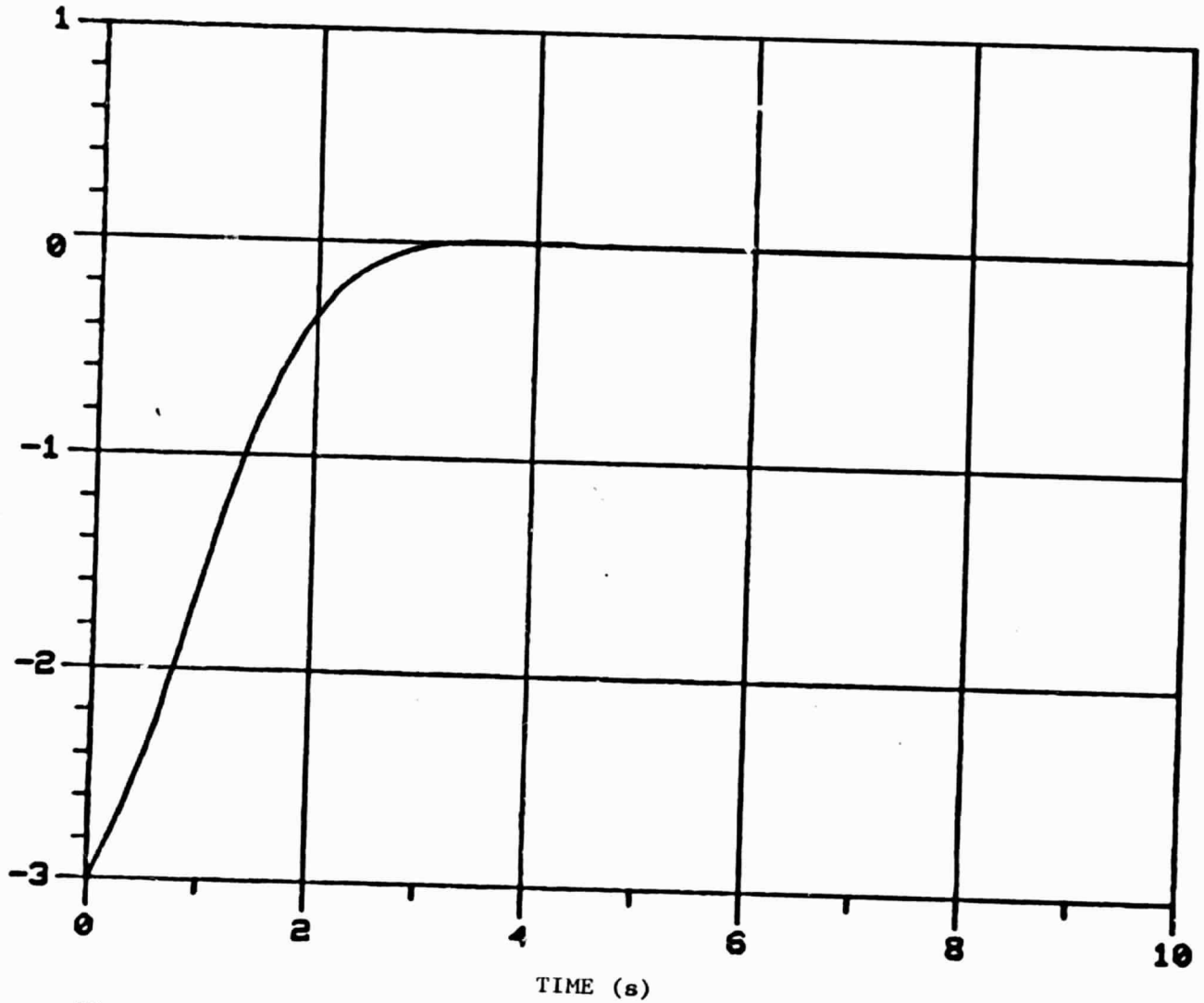

Figure 3.4 Surge Velocity Variation with VS Control for μ(o) = -3 m/s.

B

av8a.s36

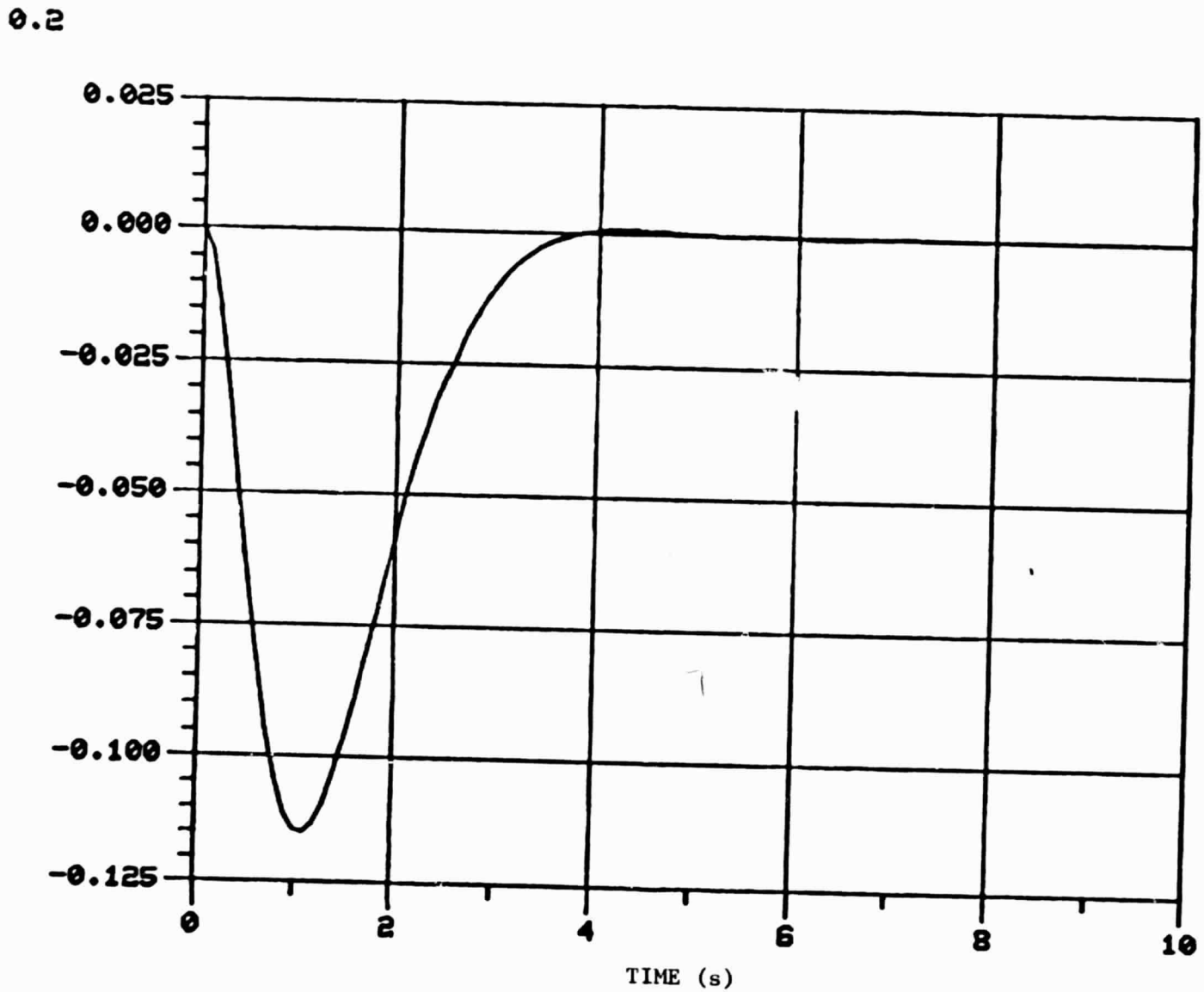

Figure 3.5 Pitch Variation with VS Control for μ(o) = -3 m/s.

D

av8a.s16

0.6

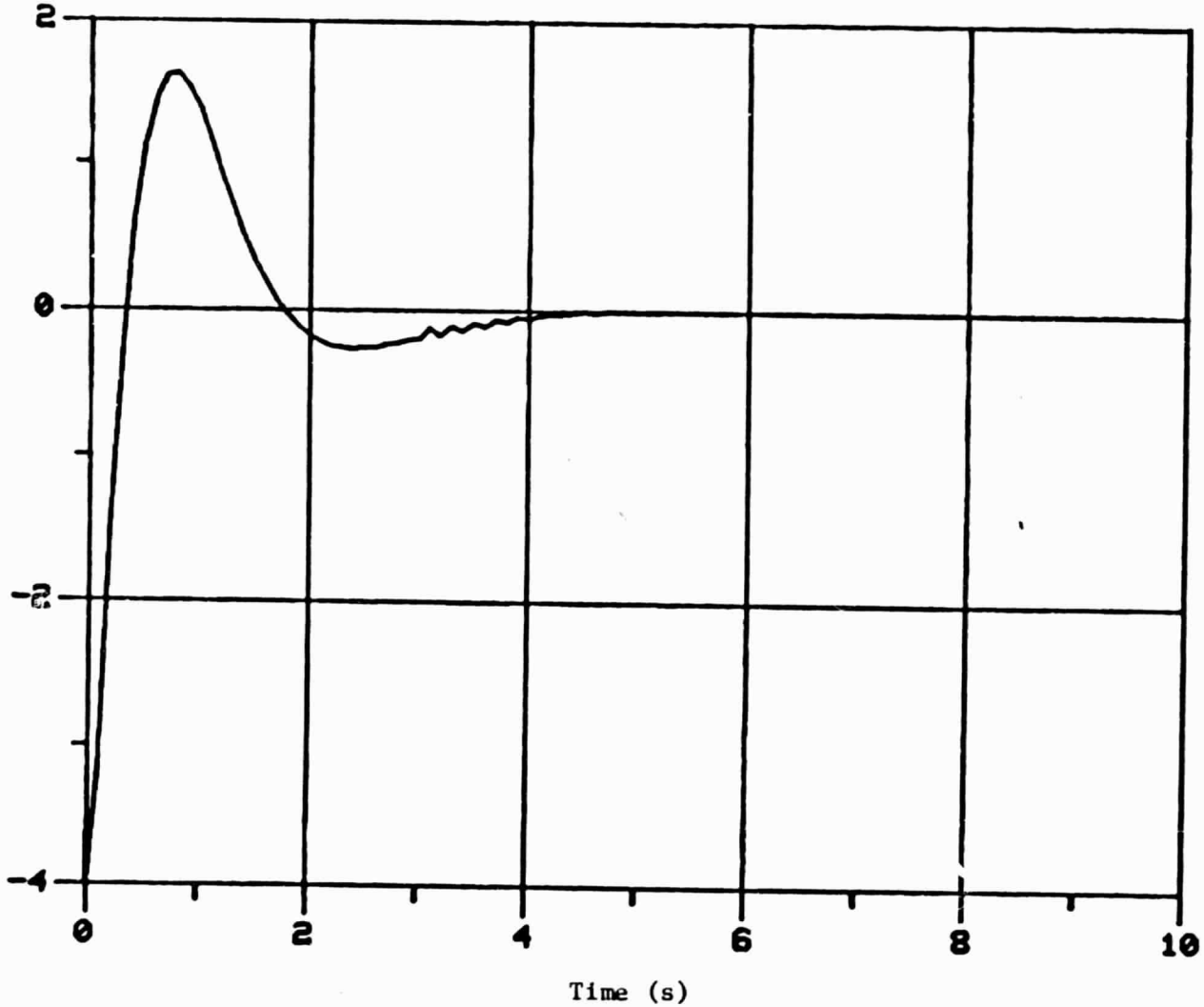

Figure 3.6 Longitudinal Stick Variation with VSS Control For $\mu(o) = -3$ m/s.

av8a.s36

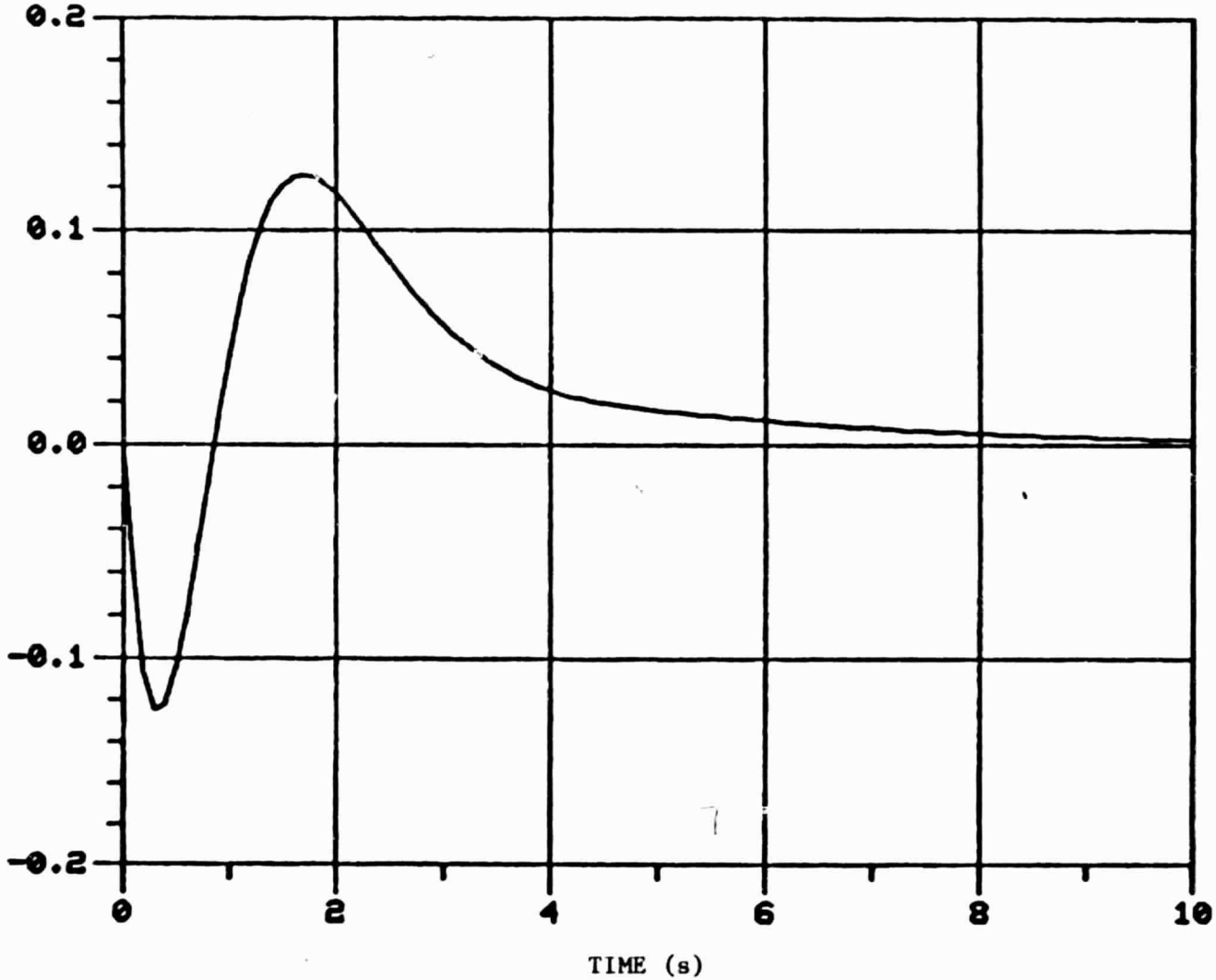

Figure 3.7 Heave Velocity with VS Control for $\mu(o) = -3$ m/s.

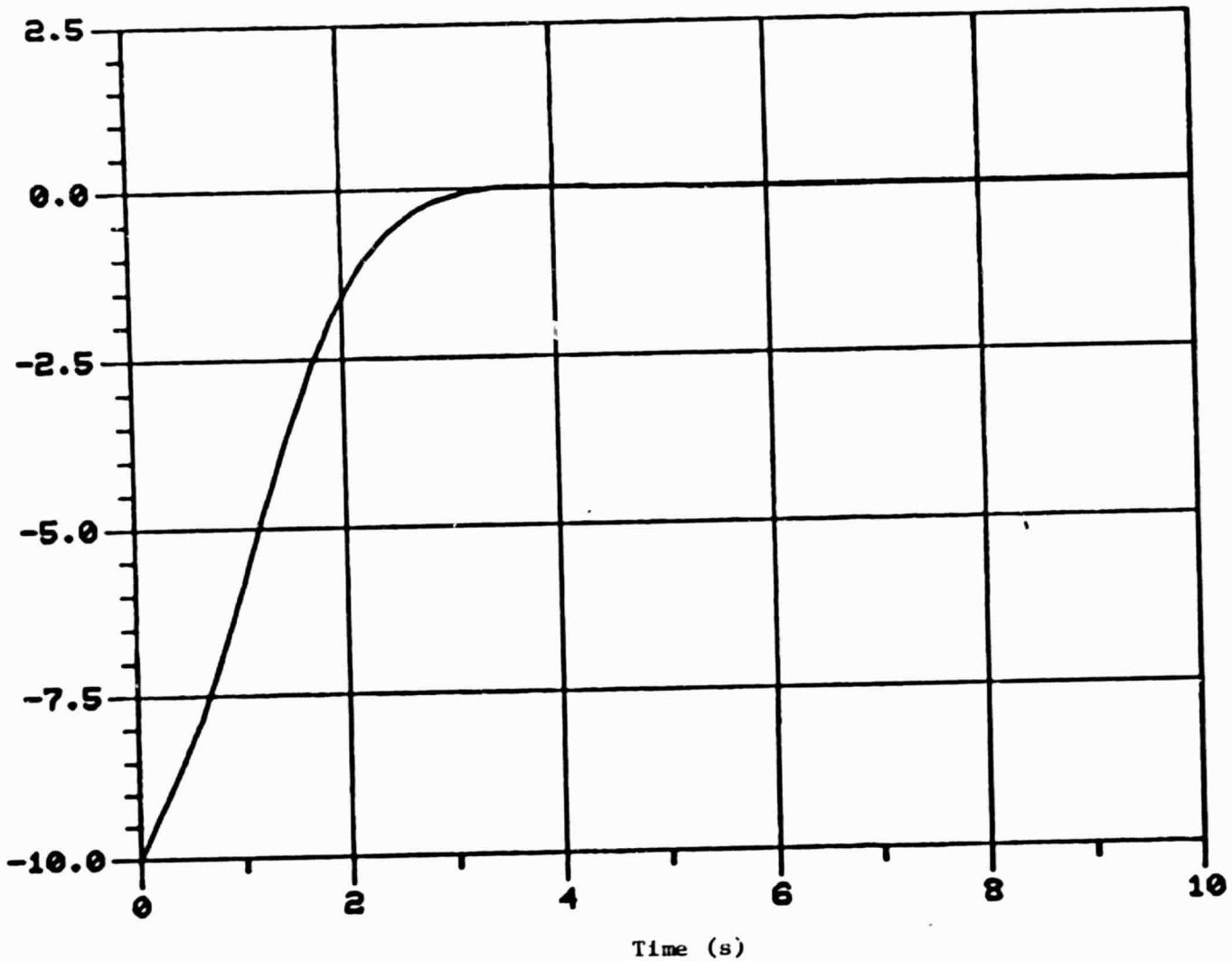

Figure 3.8 Surge Velocity Variation with VS Control for $\mu(o) = -10$ m/s.

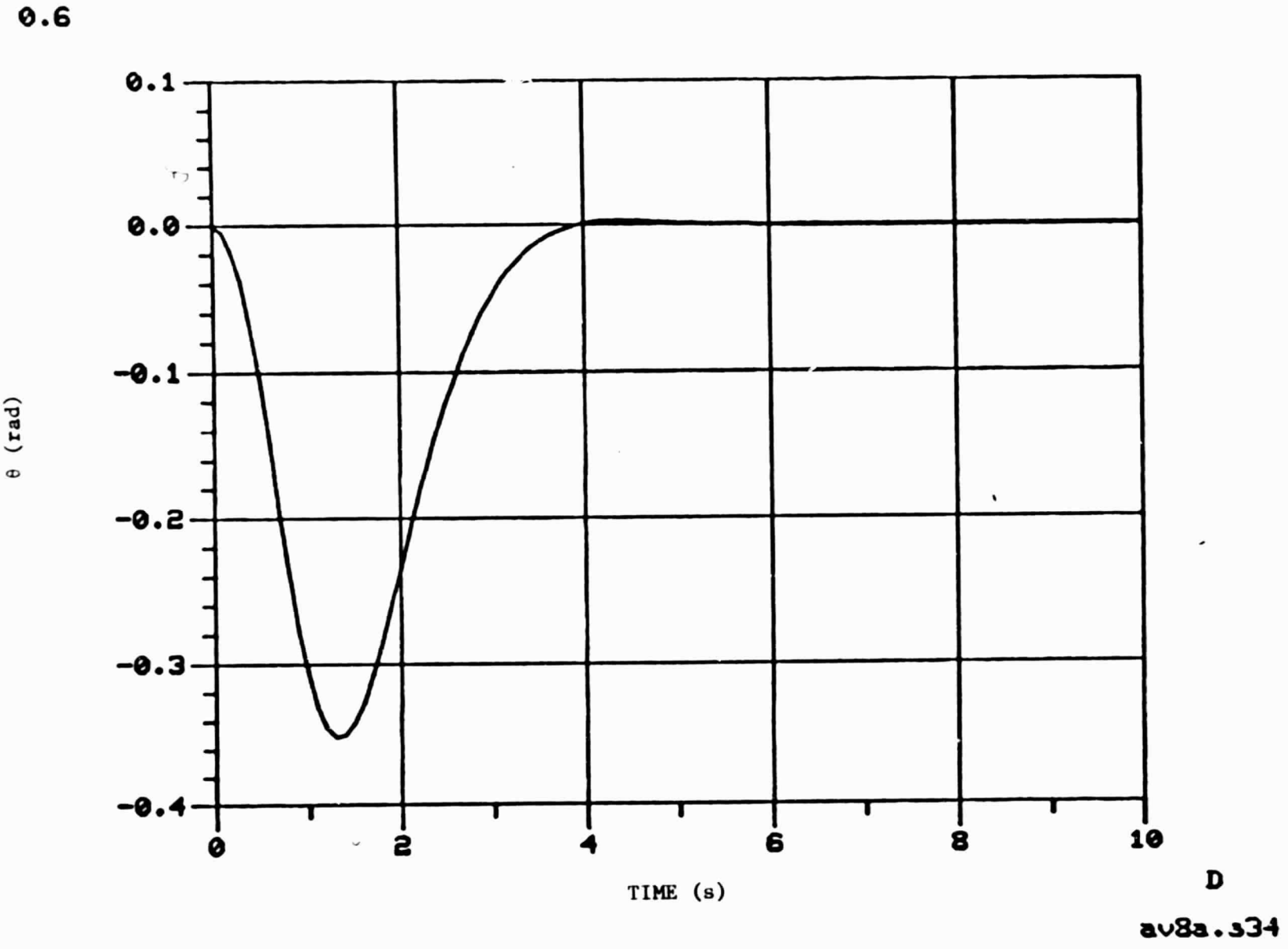

Figure 3.9 Pitch Variation with VS Control for μ(o) = -10 m/s.

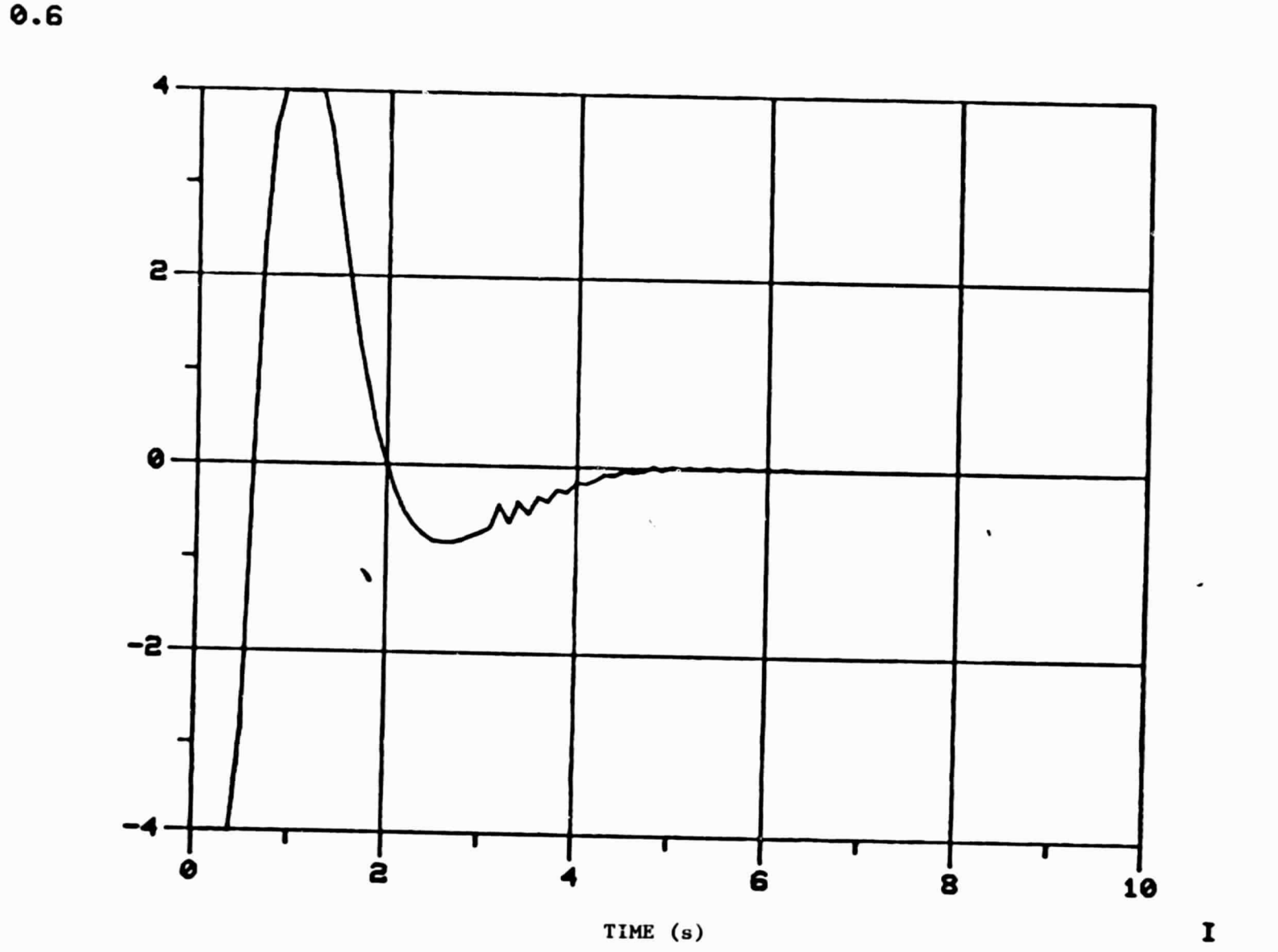

Figure 3.10 Longitudinal Stick Variation with VS Control for $\mu(o) = -10$ m/s.

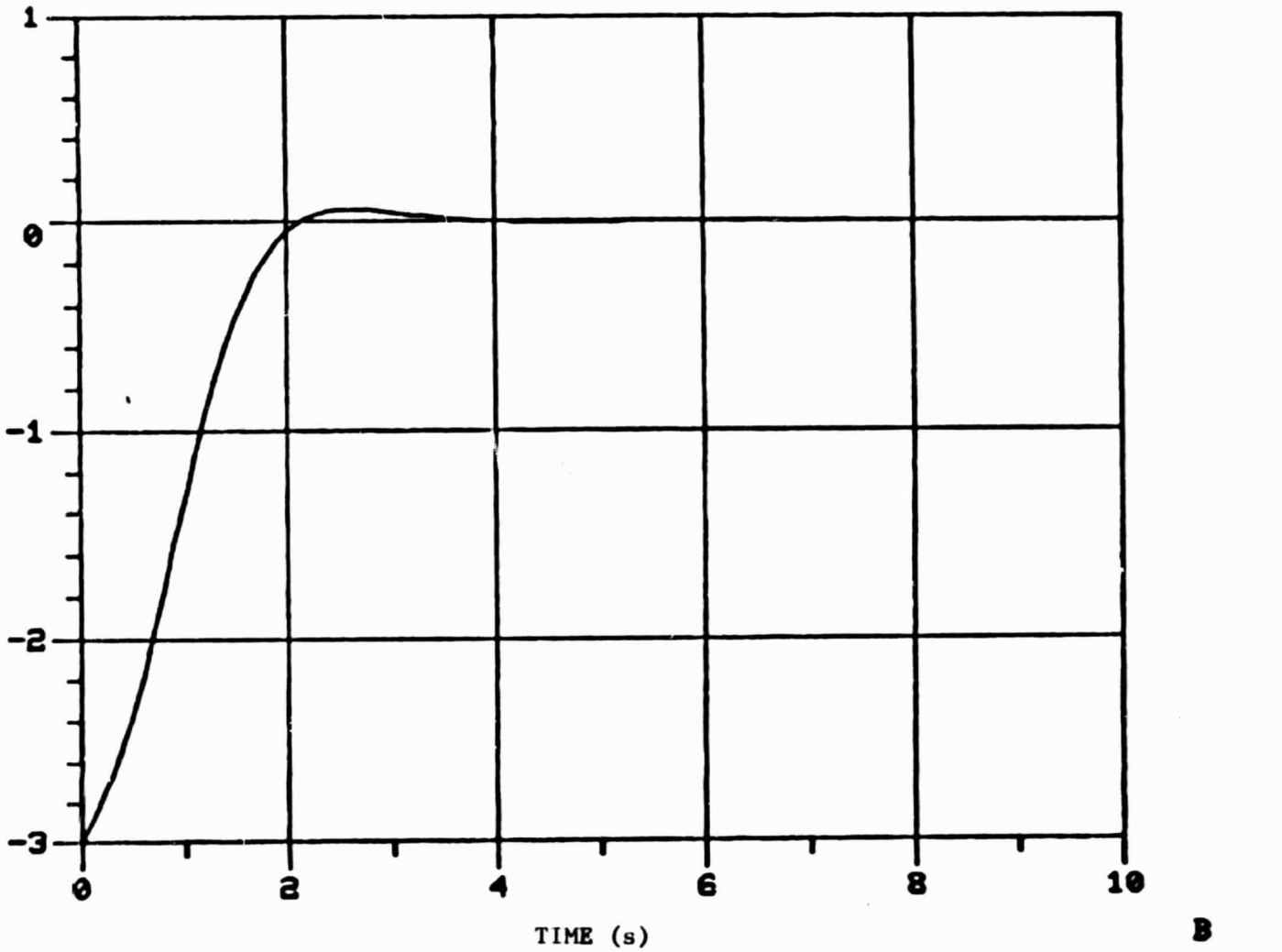

Figure 3.11 Surge Velocity Variation with Conventional Control for for $\mu(o) = -3$ m/s.

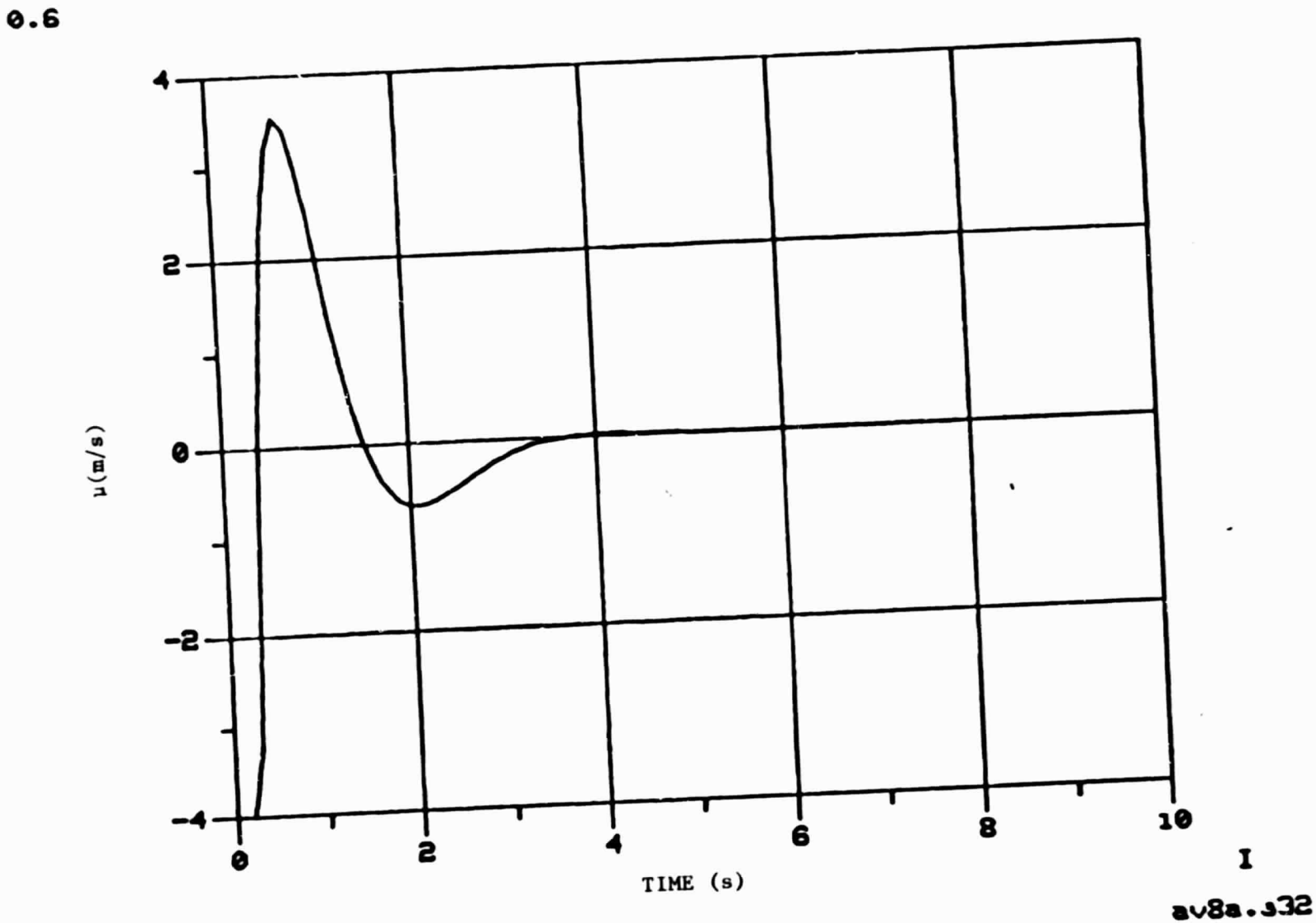

Figure 3.12 Longitudinal Stick Variation with Conventional Control for $\mu(o) = -3$ m/s.

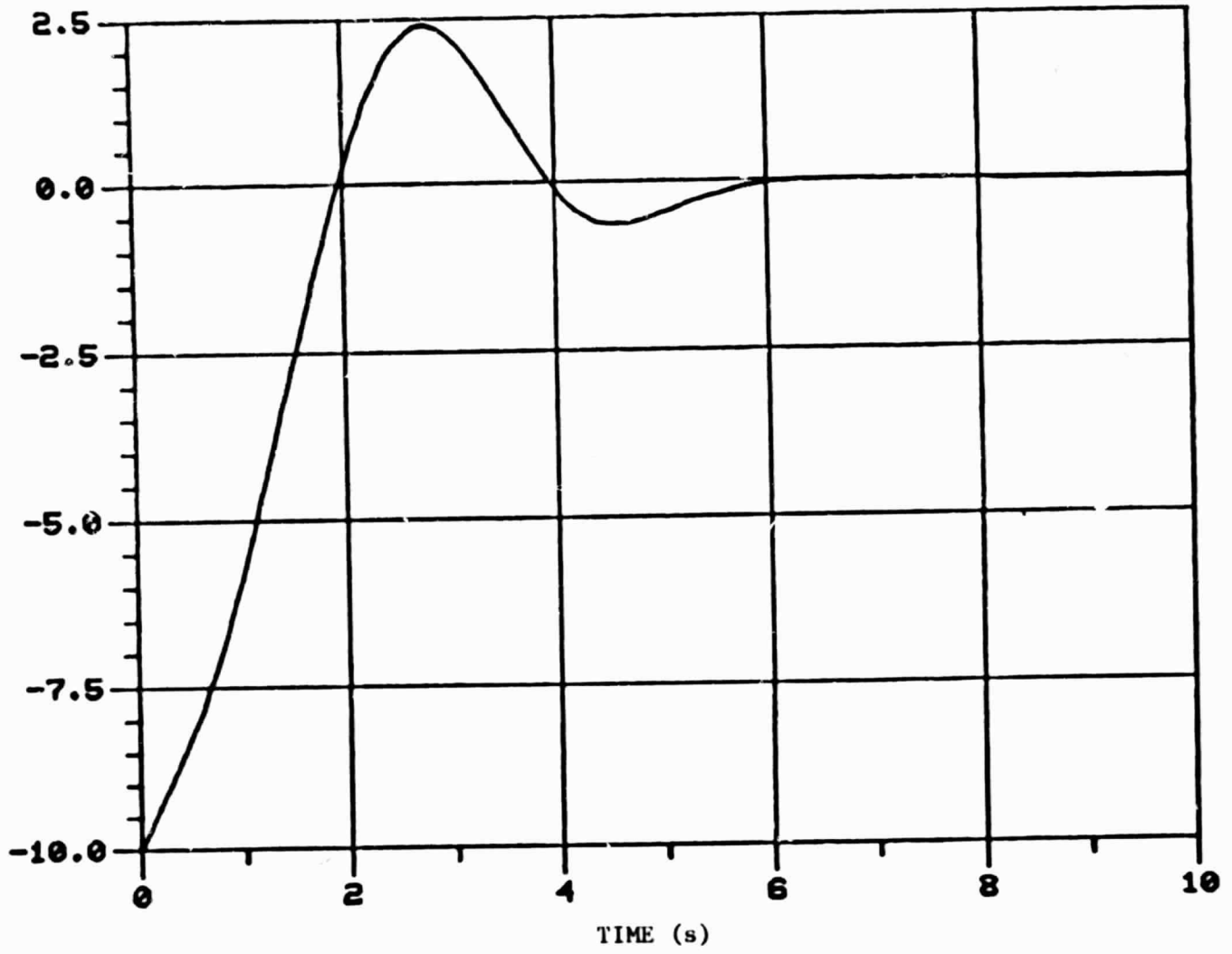

Figure 3.13 Surge Velocity Variation with Conventional Control for $\mu(o) = -10$ m/s.

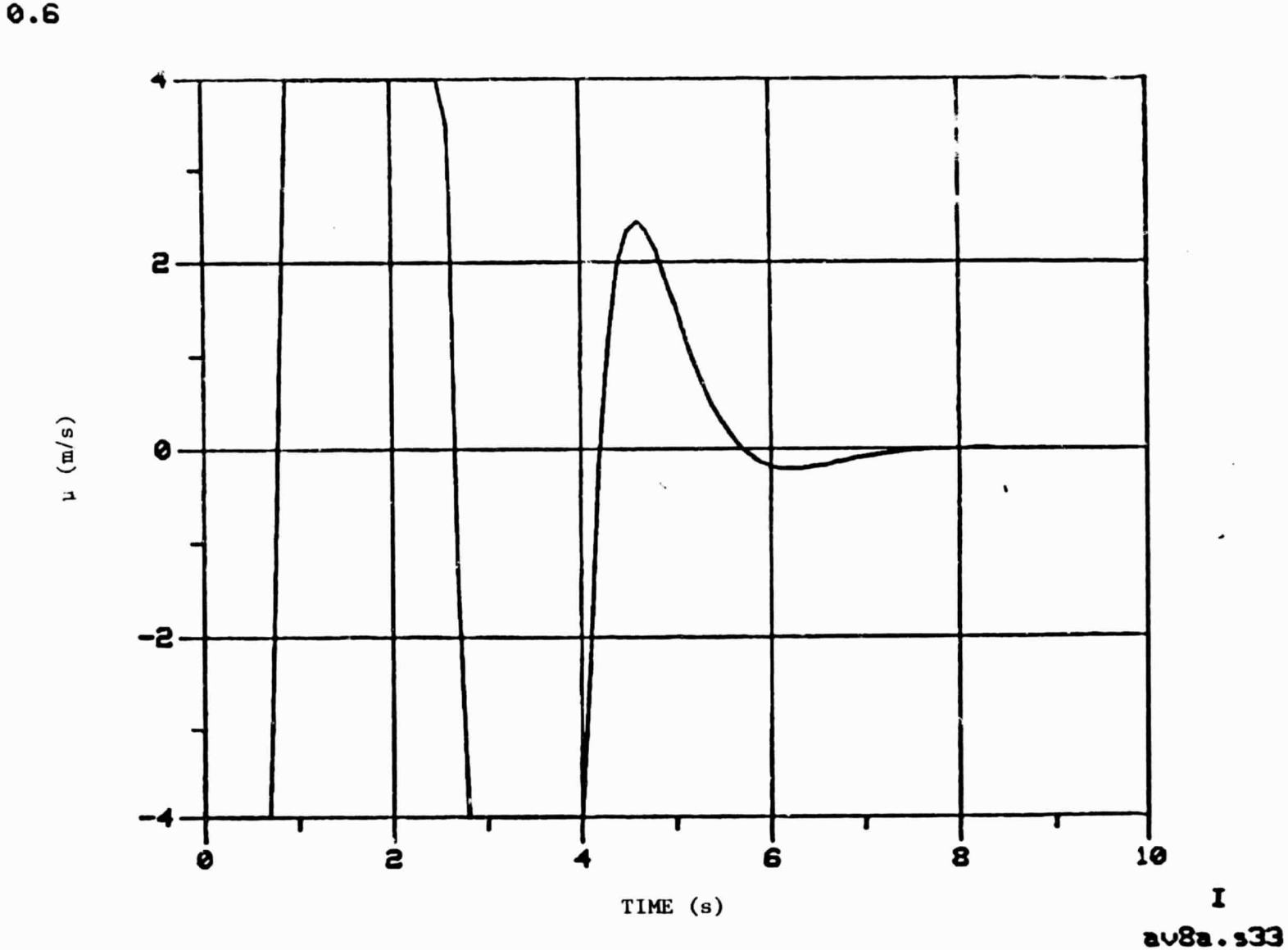

Figure 3.14 Longitudinal Stick Variation With Convention Control for $\mu(o) = -10$ m/s.

4. Future Research

The research for the next reporting period will examine the behavior of the SWJSRA and the AV-8A subject to system parameter variations and external disturbances. In addition, transient responses will be generated using nonlinear models for these aircraft. In the case of the AV-8A, we propose to examine using nozzle angle as a control to achieve reaching of the sliding surface. Currently, reaching takes up most of the transient response, and increasing k_s in the controller design leads to unstable behavior in the presence of large command inputs.

For next year, we propose to examine other aircraft types currently of interest to NASA Ames. In particular, a tail-sitter vehicle has been discussed with the technical project monitor.